MEMORANDUM REPORT BRL-MR-3830

BRL

FLIGHT TESTING FOR A 155MM BASE BURN PROJECTILE

LYLE D. KAYSER
JOHN D. KUZAN
DAVID N. VAZQUEZ

APRIL 1990

U.S. ARMY LABORATORY COMMAND

BALLISTIC RESEARCH LABORATORY
ABERDEEN PROVING GROUND, MARYLAND

NOTICES

Destroy this report when it is no longer needed. DO NOT return it to the originator.

Additional copies of this report may be obtained from the National Technical Information Service, U.S. Department of Commerce, 5285 Port Royal Road, Springfield, VA 22161.

The findings of this report are not to be construed as an official Department of the Army position, unless so designated by other authorized documents.

The use of trade names or manufacturers' names in this report does not constitute indorsement of any commercial product.

REPORT DOCUMENTATION PAGE

Form Approved
OMB No. 0704-0188

1. AGENCY USE ONLY (Leave blank)	2. REPORT DATE	3. REPORT TYPE AND DATES COVERED
	April 1990	Memorandum, Jun 88 - Dec 89

4. TITLE AND SUBTITLE

Flight Testing for a 155mm Base Burn Projectile

5. FUNDING NUMBERS

PR: 1L162618AH80

6. AUTHOR(S)

Lyle D. Kayser, John D. Kuzan, and David N. Vazquez

7. PERFORMING ORGANIZATION NAME(S) AND ADDRESS(ES)

8. PERFORMING ORGANIZATION REPORT NUMBER

9. SPONSORING/MONITORING AGENCY NAME(S) AND ADDRESS(ES)

Ballistic Research Laboratory
ATTN: SLCBR-DD-T
Aberdeen Proving Ground, MD 21005-5066

10. SPONSORING/MONITORING AGENCY REPORT NUMBER

BRL-MR-3830

11. SUPPLEMENTARY NOTES

This report supersedes BRL-IMR-915 dated December 1988.

12a. DISTRIBUTION/AVAILABILITY STATEMENT

Approved for public release; distribution is unlimited.

12b. DISTRIBUTION CODE

13. ABSTRACT (Maximum 200 words)

A modified 155mm M864 base burn projectile was used to obtain in-flight measurements of pressure and temperature in the base region of the projectile. The M864 uses the base burn concept of reducing base drag by injecting gas, generated by burning propellant, into the base area. One measurement of pressure and one of temperature was made in the chamber where the propellant is burned; pressure was measured in two locations on the base of the projectile. Pressure was also measured near the nose of the projectile, and a yawsonde was used to measure projectile yaw. Data illustrates the increased base pressure that occurs while the propellant is burning, along with fluctuations in pressure due to projectile yawing motion.

14. SUBJECT TERMS

Projectiles, Base Burning, Base Bleed, Base Pressure (3L)

15. NUMBER OF PAGES

40

16. PRICE CODE

17. SECURITY CLASSIFICATION OF REPORT	18. SECURITY CLASSIFICATION OF THIS PAGE	19. SECURITY CLASSIFICATION OF ABSTRACT	20. LIMITATION OF ABSTRACT
UNCLASSIFIED	UNCLASSIFIED	UNCLASSIFIED	SAR

GENERAL INSTRUCTIONS FOR COMPLETING SF 298

The Report Documentation Page (RDP) is used in announcing and cataloging reports. It is important that this information be consistent with the rest of the report, particularly the cover and title page. Instructions for filling in each block of the form follow. It is important to *stay within the lines* to meet *optical scanning requirements*.

Block 1. Agency Use Only *(Leave blank)*.

Block 2. Report Date. Full publication date including day, month, and year, if available (e.g. 1 Jan 88). Must cite at least the year.

Block 3. Type of Report and Dates Covered. State whether report is interim, final, etc. If applicable, enter inclusive report dates (e.g. 10 Jun 87 - 30 Jun 88).

Block 4. Title and Subtitle. A title is taken from the part of the report that provides the most meaningful and complete information. When a report is prepared in more than one volume, repeat the primary title, add volume number, and include subtitle for the specific volume. On classified documents enter the title classification in parentheses.

Block 5. Funding Numbers. To include contract and grant numbers; may include program element number(s), project number(s), task number(s), and work unit number(s). Use the following labels:

C	- Contract	PR	- Project
G	- Grant	TA	- Task
PE	- Program Element	WU	- Work Unit Accession No.

Block 6. Author(s). Name(s) of person(s) responsible for writing the report, performing the research, or credited with the content of the report. If editor or compiler, this should follow the name(s).

Block 7. Performing Organization Name(s) and Address(es). Self-explanatory.

Block 8. Performing Organization Report Number. Enter the unique alphanumeric report number(s) assigned by the organization performing the report.

Block 9. Sponsoring/Monitoring Agency Name(s) and Address(es). Self-explanatory.

Block 10. Sponsoring/Monitoring Agency Report Number. *(If known)*

Block 11. Supplementary Notes. Enter information not included elsewhere such as: Prepared in cooperation with ...; Trans. of...; To be published in.... When a report is revised, include a statement whether the new report supersedes or supplements the older report.

Block 12a. Distribution/Availability Statement. Denotes public availability or limitations. Cite any availability to the public. Enter additional limitations or special markings in all capitals (e.g. NOFORN, REL, ITAR).

- DOD - See DoDD 5230.24, "Distribution Statements on Technical Documents."
- DOE - See authorities.
- NASA - See Handbook NHB 2200.2.
- NTIS - Leave blank.

Block 12b. Distribution Code.

- DOD - Leave blank.
- DOE - Enter DOE distribution categories from the Standard Distribution for Unclassified Scientific and Technical Reports.
- NASA - Leave blank.
- NTIS - Leave blank.

Block 13. Abstract. Include a brief *(Maximum 200 words)* factual summary of the most significant information contained in the report.

Block 14. Subject Terms. Keywords or phrases identifying major subjects in the report.

Block 15. Number of Pages. Enter the total number of pages.

Block 16. Price Code. Enter appropriate price code *(NTIS only)*.

Blocks 17. - 19. Security Classifications. Self-explanatory. Enter U.S. Security Classification in accordance with U.S. Security Regulations (i.e., UNCLASSIFIED). If form contains classified information, stamp classification on the top and bottom of the page.

Block 20. Limitation of Abstract. This block must be completed to assign a limitation to the abstract. Enter either UL (unlimited) or SAR (same as report). An entry in this block is necessary if the abstract is to be limited. If blank, the abstract is assumed to be unlimited.

Table of Contents

INTENTIONALLY LEFT BLANK.

List of Figures

INTENTIONALLY LEFT BLANK.

I. Introduction

Of the three components of drag affecting a projectile in flight, base drag frequently accounts for one-half or more of the total drag. Base drag results from the low pressure associated with the wake and the region of separated flow behind the projectile. One method of reducing base drag is to increase the pressure in the base region through low velocity mass injection into the wake. In the 155mm M864 base burn projectile, mass injection is in the form of gas generated from burning solid propellant.

The solid propellant is housed in a propellant chamber located at the base of the projectile and the mass injection occurs through a hole in the chamber. The hole is not a nozzle, such as that found in a rocket-assisted projectile, so that the thrust resulting from the burning propellant is small.

Accurate measurements and numerical models are uncommon for base flows, owing to their complexity; hence, systems which reduce base drag are difficult to design. In spite of this, the 155mm M864 uses a base burn system successfully for extending its range. However, modeling efforts and system performance would benefit from in-flight measurements of temperature and pressure in the projectile propellant chamber and base region, and this is the purpose of present work.

The design of the in-flight instrumentation system was based upon flight tests where forebody and transonic surface pressures were measured successfully and compared to computed data.[1] In addition, ground tests[2] of the base pressure measurement system were performed to insure that the design was sound.

The resulting system was contained in the body of an M864 projectile; however, the test projectile weight and inertial properties did not match those of the M864. Four measurements of pressure were made: two on the projectile base, one in the propellant chamber, and one on the projectile ogive. Temperature was measured in the propellant chamber and projectile yaw was measured with a yawsonde. [3] The signals from the various measurements were telemetered back to a ground receiving station.

This work was supported by the Project Manager, Cannon Artillery Weapon Systems (PMCAWS) and the U.S. Army Research Development and Engineering Center (ARDEC), Picatinny Arsenal, New Jersey.

[1] *Kayser, L.D., Clay W.H., D'Amico W.P., "Surface Pressure Measurements on 155mm Projectile in Free-Flight at Transonic Speeds," ARBRL-MR-3534, Ballistic Research Laboratory Memorandum Report No. 3534, July 1986.*

[2] *Kayser, L.D., Kuzan, J.D., Vazquez, D.N., "Ground Testing for Base-Burn Projectile Systems," BRL-MR-3708, Ballistic Research Laboratory Memorandum Report No. 3708, November 1988. AD No. A201107*

[3] *Mermagen, W.H., Clay, W.H., "The Design of a Second Generation Yawsonde," BRL-MR-2368, Ballistic Research Laboratory Memorandum Report No. 2368, April 1974 AD No. 780064*

II. Experiment

The experimental apparatus consisted of an M864 155mm base-burn projectile instrumented to telemeter selected pressure, temperature, and projectile yawing motion measurements; a ground-based telemetry receiving station; a M199 155mm gun system; a smear camera; a HAWK Doppler velocimeter; and a Weibel radar system. Figure 1 shows the gun system and most of the experimental apparatus in place at the firing location. For this paper, the instrumented projectile and the receiving station will be discussed.

In order to make pressure measurements in the propellant chamber and at the projectile base, holes of 2.0mm (5/64 inch) diameter were drilled in the walls of a standard M864 projectile base assembly, forming paths for pressure in one location to be sensed at another location. Figure 2 is a sketch of the base assembly and instrumentation canister, which also shows the paths for pressure at the orifices in the base area to be sensed by their respective pressure transducers. Each path was made in several segments by drilling holes with split point drills; sections of the holes were then plugged by welding to provide a leak free path from the orifice to the transducer, as shown in Figure 2.

Since the base assembly is made in two halves, it was necessary to form a leak free path across their threaded joint through careful alignment of the holes and the use of small O-ring seals. The alignment was secured by placing three set screws through the threaded section at circumferential positions between the pressure paths. Figure 2 also shows the location of the different orifice positions and their circumferential locations; Figure 2 is not a true cross sectional view.

The pressure transducers used in these experiments were purchased from the Kulite Corporation and are miniature, solid-state semiconductor strain-gage sensors with a four element bridge circuit. The transducers are rated for 25 psia full scale; however, they are equipped with mechanical stops for an overload protection of 40 times the rated pressure. The transducer sensitivity to acceleration is very low and is quoted to be typically 0.0005% of full scale per "g" perpendicular to the diaphragm and 0.0001% transverse to the diaphragm. Within the gun tube, maximum projectile accelerations were on the order of 6000 g, but during flight and data acquition accelerations were less than 3 g.

A hole was drilled through the transducer fixture and the front wall of the base assembly so that a thermocouple could be inserted into the propellant chamber. A tungsten, tungsten-rhenium thermocouple was used to measure temperature inside the propellant chamber. A slightly non-constant cold junction temperature of approximately 80° F inside the instrumentation canister was considered adequate for the much higher temperatures to be measured.

In order to protect the pressure transducers from the extreme pressures during the launch, a "pusher plate" was fabricated out of propylux to fit over the projectile base during launch. A seal was affected between the projectile base and the pusher plate with RTV molded to conform to both. The RTV was approximately 1/4 of an inch thick. Figure 3 shows the lower half of the projectile base assembly, the pusher plate and the RTV seal. Small brass disks were inserted in the RTV seal to cover the pressure path orifices to insure that no RTV was extruded into the pressure paths. A seal was affected

in the chamber pressure orifice with a brass fitting filled with magnesium-teflon. It was thought that the propelling charge would ignite the magnesium-teflon, which would burn for approximately 0.25 seconds, and once burned would open the pressure orifice.

The propellant grain used in the M864 is in two monolithic halves, which are separated by small spacers when in the projectile. Figure 4 shows the two halves. Figure 5 shows a cross section of the base with propellant grain and the two magnesium-teflon ignitors installed . The magnesium-teflon ignitors are designed to burn for two seconds and insure propellant burning which could be snuffed during the muzzle exit decompression. The weight of the propellant grain is 1.17 kg and the ignitors are approximately .02 kg.

The circuit boards, depicted in Figure 2, and batteries for powering the electronics were mounted inside the instrumentation canister above the transducers. (Reference 1 explains many of the details involved in making in-flight pressure measurements and telemetering the results back to earth.) The circuit boards contained a voltage regulator which supplied power to the transducers and signal outputs were amplified by a factor of approximately 30. Voltage controlled oscillators, with different center frequencies for each output, were used to convert signal voltages to frequency data. A timer and switching device that shorted the output of the gages for 40 msec at 15 sec intervals was also provided in the circuit. The primary purpose in shorting the gages was to track any zero shift in the circuit. The frequency data from the the VCO's were mixed and passed to the nose section of the projectile through a single conductor, ultimately to be broadcast back to the receiving station.

The ogive of the projectile contained a pressure transducer which sensed the pressure on the forebody of the projectile as shown in Figure 6. Solar sensors, mounted in the ogive flush to the exterior of the projectile, were used as the sensing device of a yawsonde that measured projectile yawing motion. The voltage signals from the yawsonde and the forebody pressure transducer were amplified, converted to modulated frequencies, and then mixed with the signals from the base of the projectile. All of the mixed frequency signals were then used to modulate a transmitter carrier frequency of 250 Mhz. The signal broadcast from the projectile was received by antennas on the ground near the launch site and recorded on magnetic tape. The analog signals were later digitized and stored on a VAX 11/780 for data reduction and analysis.

Figure 7 is a schematic of the entire projectile which shows the location of measurements and other pertinent components. As stated previously, there were two pressure measurements on the projectile base, pressure and temperature measurements in the propellant cavity, and pressure and solar sensor measurements on nose section. The projectile weight, without propellant grain and mag-teflon ignitors, was 37.3 kg compared to 45.5 kg for the M864. Axial and transverse moments of inertia were respectively 0.1378 and 1.579 $kg \cdot m^2$ compared to 0.1557 and 1.569 for the M864. The center of gravity was 0.319m from the base compared to 0.314m for the M864. At launch, the gun elevation angle was set at 850 mils and the muzzle velocity was 447 m/sec (Mach 1.30). The rifling twist of one turn in 20 calibers gave a spin rate of 144 rev/sec. The atmospheric pressure was 769 mm Hg and the temperature was 295k (71 deg F.).

A smear camera photographed the projectile near the exit of the gun tube as a check of projectile integrity. A Weibel radar was used to obtain projectile muzzle velocity; a HAWK Doppler Velocimeter was used to obtain projectile velocity throughout the trajectory.

III. Results and Discussion

Base pressure, chamber pressure, chamber temperature, and nose cone pressure data are shown in the remaining figures. Some yawsonde data were received, but because of difficulties encountered with the solar sensors no yawsonde data are presented. The yaw of the projectile was small, however.

Figure 8 shows the pressure at the small recessed radius (base corner) of the base. The pressure is made dimensionless using the constant value of sea level atmospheric pressure. The predominant trend of the data is due to altitude changes which are indicated by a decreasing pressure on the up-leg portion of the trajectory and increasing pressure on the down-leg. The apparent noisyness of the data is primarily due to the projectile spin and yawing motion and will be examined in more detail later. The initial pressure rise from zero to 1.5 seconds results as the propellant reaches steady state burning. At about two seconds, the decreasing atmospheric pressure dominates the trend of the data. At 6-7 seconds, the discontinuity in the curve is caused by the transition from supersonic to subsonic velocity. The pressure reaches a minimum at apogee, which occurs at about 28 seconds. Another discontinuity occurs at 35-36 seconds and coincides with propellant burnout.

Data from the two base pressures, chamber pressure, and nose cone pressure are shown in Figure 9. The data were filtered to remove most of the spin and yaw oscillations and to make comparisons easier. The two base pressures are seen to be nearly equal for most of the burn phase; but, as burnout occurs, the pressures diverge and the pressure at the corner is consistently lower than that on the flat area. A pyrotechnic protection device, which was designed to protect the chamber pressure transducer from high pressure gun gases, opened up at about 3.5 seconds. The abrupt pressure drop shows that the transducer quickly responded to the chamber pressure which then followed a path about 5% higher than the base pressures. The pyrotechnic protection should have burned out within 0.25 second, but it is speculated that movement of the propellant grain occurred during launch and prevented immediate ignition. At 21-22 seconds, a pressure spike occurs indicating a substantial increase in gas generation due to burning. The specific mechanism or event which caused this increase is not understood, but it was also observed in the temperature measurement to be shown later. The nose cone pressure is also seen to be dominated by changes in pressure due to altitude. At about 44 seconds into the flight, the nose pressure shows a discontinuity which is not yet understood.

Figures 10, 11, and 12, show pressure data divided by the free-stream static pressure, which provides a more conventional dimensionless parameter than the constant value of the two previous figures. The predominant trends of the data are now due to the propellant gas and the aerodynamics of projectile base flow rather than altitude changes over the trajectory. Again, the initial pressure rise (see Figures 10,and 11) seen at the base corner

and base flat is a result of the propellant ignition delay or process [4] and the time that is required for propellant deflagration to reach a steady state. Figure 12 indicates that the delay, until full burning occurs, is about 1.5 seconds into the flight. At about two seconds, there is a small pulse and sudden decrease in pressure, which is thought to coincide with the depletion of the magnesium-teflon ignitors. Since the ignitors are providing additional gas injection, a slight decrease in pressure level following burnout is expected. It is estimated the mass injection rate from the ignitors is about one fifth of the average injection rate from the propellant. This sudden decrease, occurring at the end of the initial pressure rise, gives the appearance of a pressure pulse in Figures 10 and 11. At approximately 6 seconds, the discontinuities seen in Figures 10, 11 and 12 result from the transition to subsonic velocity. Other discontinuities for the three pressures, Figures 10 and 11, coincide near 35 seconds which is evidence of propellant burnout; note that the discontinuity is less severe at the base corner. During the burn phase, the two pressures are nearly equal; but, after propellant burnout, the pressure at the base corner becomes lower than the pressure at the base flat. In a recirculating base flow, a local stagnation region would be expected near the center of the projectile base along with a higher pressure. This higher pressure near the center suggests a pressure gradient that has the qualitative trend of the experimental data which show a lower pressure at the base corner. During the base burn, the propellant gas appears to relieve the pressure gradient across the base.

Figure 11, which is an expanded view of Figure 10, shows the propellant burn maintaining a near constant, or slightly increasing, pressure in the chamber until approximately 27 seconds. After this time the propellant grain begins a regressive burn (the grain provides less surface area for burning) until there is no more propellant at about 35 seconds, and the chamber pressure is nearly the same as the base flat pressure.

Figure 12 shows the base corner pressure, along with wind tunnel measurements of base pressure[5] and some computations of base pressure. Wind tunnel measurements, made on a typical projectile with and without a boattail, confirm the discontinuity in base pressure found in the transonic regime. Computations[6] for an M864 Projectile base without base burn (mass injection) show reasonable agreement with the trend of the experimental data near launch (time=zero). A computation with base burn (mass injection) is seen to predict an increases in base pressure. A direct comparison of the base burn pressures for the computation and the experiment cannot be made since the computational parameters did not exactly match those of the experiment. For example, the computation is for a perfect gas with heated air (2300° F) as the injected material and mass injection rates are difficult to match due to the transient nature of the experiment. Also, temperature data, to be discussed later, may indicate that the value of 2300° F is too low.

In order to see some of the effects of Mach number on base pressure, and, fortuitously, the effect of base burn on base pressure at different Mach numbers, Figure 13 was produced. This was accomplished by using the HAWK Doppler velocimeter data, which gives the velocity of the projectile over the trajectory (*i.e.*, versus time), and the base pressure

[4] *Kuzan, J.D., Oskay, V., "Ignition Delay of the Solid Propellant in the M864 Base Burn Projectile," BRL-MR-3653, Ballistic Research Laboratory Memorandum Report No. 3653, March 1988 AD No. B121544*

[5] *Kayser, L.D. "Base Pressure Measurements on a Projectile Shape at Mach Numbers from 0.91 to 1.20," ARBRL-MR-03353, Ballistic Research Laboratory Memorandum Report No. 03353, April 1984 AD No. A141341*

[6] *Nietubicz, C. J. "unpublished data," U.S. Army Ballistic Research Laboratory, 1988.*

histories presented earlier. If the trajectory of the projectile is considered, the graph can be read from right to left beginning at a Mach number of 1.26 where the pressure is increasing due to the base burn propellant. The spike in the pressure curve near Mach number 1.19 is the magnesium-teflon ignitor burnout. Again, the discontinuity in pressure resulting form the transition to transonic speed is seen. Pressure at the base gradually increases to a level slightly above the free-stream static pressure. Base pressures at transonic or high subsonic speeds can be very close to free-stream static pressures and the injection of propellant gas apparently pushes the pressure level above the local ambient (free-stream static) pressure. After the projectile reaches apogee (marked on the figure), it accelerates toward earth; the curve now advances left to right. Shortly after going through the apogee, the propellant burnout phase occurs and there is a dramatic reduction in the base pressure. Until this time the pressure in the base corner and the base flat were nearly equal (to within experimental error), but now the two differ as a result of the base pressure gradient. Splashdown occurs near a Mach number of 0.85.

Figure 14 shows the chamber pressure from the in-flight test compared to the chamber pressure measured in the ground tests of Reference 1 at a spin rate near the range of the in-flight measurement and with no spin. For the ground tests, the pressure data were made dimensionless using the atmospheric pressure, which was assumed to be equal to the exit pressure. For the flight tests, the pressure on the base flat is close to the throat exit and is assumed to be a good approximation to the exit pressure. It is therefore used to compute a dimensionless chamber pressure for this figure. The effect of spin is clearly seen in the ground test results; at zero spin rate the propellant burns for roughly 40 seconds, while at a spin rate of 142 revolutions per second (rps) the propellant burns for only 28 seconds. In the flight test, the projectile initially has a spin rate of 143 rps and slows to 120 rps near burnout. This decrease in spin rate accounts for some percentage of the increased burn time found in the in-flight test, where the burn time is about 35 seconds. Another factor which would dictate a longer burning time is the lower pressure environment encountered at higher altitudes. Miller[7] has demonstrated, in strand burner experiments, that the propellant burning rate decreases with decreasing pressure.

Figure 15 shows the chamber temperature from the present test compared to the chamber temperature measured in the ground tests of Reference 1 at two different spin rates. Note that in the ground tests, as spin rate increases, the thermocouple indicates a temperature increase. It is speculated that this increase is due to increased vibration keeping the thermocouple cleaner, rather than the temperature of the burning propellant increasing as the spin rate increase. Similarly, the in-flight temperature is higher still. It is suggested that this higher temperature, and the large temperature fluctuations, are due to the yawing motion of the projectile which causes vibration of the thermocouple. This vibration may result in periodic shedding of propellant residue, which inhibits heat transfer, and indirectly produces an erratic temperature history. Near burnout there is a brief interruption of the rapid temperature decrease for both the in-flight and ground tests. This may be due to ignition or burning of the rubber coating around the propellant grain (see Figure 4) as the propellant is depleted.

[7] *Miller, M.S., and Holmes, H.E., "An Experimental Determination of Subatmospheric Burning Rates and Critical Diameters for AP/HTPB Propellant," Ballistic Research Laboratory Memorandum Report No. 3719, December 1988*

Figure 16 is a comparison of the chamber temperature and pressure. The pressure was adjusted by multiplication a factor so that it could be plotted on the same figure and still retain its qualitative character. The event near 22 seconds, previously shown in the pressure data, coincides with the large spike in the temperature data. This coincidence is evidence that a physical event has occurred and the spike is not the result of noise in the data. This transient event may have cleaned the thermocouple as evidenced by a brief temperature rise to about 4000° F. The temperature is thought to give a positive indication of when the propellant is expended, since there is a dramatic drop in the temperature, with a short rise as the coating begins to burn. The pressure requires very little time to equilibrate with the ambient pressure and the discontinuity in the pressure curve occurs just prior to the start of the temperature inflection.

Most of the pressure data of the previous figures were filtered and, therefore, show trends of slowly changing parameters such as Mach number and altitude. Some of the following data were also filtered, but cutoff frequencies were selected so that effects of projectile motion could be examined. Data show the effects of spin at frequencies on the order of 140 Hz and also the effects of fast mode coning on the order of 10 Hz. Data have not yet been examined in sufficient detail to isolate the effects of the slow mode coning frequency, but it should be possible to determine the amplitude of the slow mode arm.

Figure 17 shows unfiltered nose cone data and unfiltered pressure at the base corner. The nose cone pressure shows a high frequency, about 140 Hz, oscillation primarily due to the spin of the projectile. This higher frequency is modulated as a result of the projectile fast mode coning and the rate is seen to be about 7 rps. The higher frequency, on the average, occurs at a frequency equal to the difference between the spin rate and the slow mode coning rate. The maximum amplitude of the 'spin' oscillation in a fast mode coning cycle represents the pressure at a yaw angle which is equal to the sum of the fast and slow mode arms and the minimum amplitude corresponds to the pressure at a yaw angle equal to the difference between the slow and fast mode arms.

Figure 18 shows the early nose cone pressure with the time scale highly expanded. At about 0.03 second (30 milliseconds), it appears that a realistic pressure is being measured and by 40-50 milliseconds the pressure measurement indicates a stabilized pattern. The launch velocity was approximately 450 m/sec. Therefore at 50 milliseconds, the projectile would be about 18 meters from the gun muzzle.

The pressure at the base corner, also shown in Figure 17 shows a cyclic pattern at a frequency corresponding to that of the modulated nose cone pressure. A faster frequency mode corresponding the 'spin' frequency also exists, although it is not clear from this figure. If we consider the averaged data with the spin effect removed, the higher base pressure is seen to occur when modulation of the nose pressures indicates a smaller projectile yaw. Figure 19 shows both base pressures with the spin effect filtered out. Both base pressures are seen to be nearly equal in magnitude. This figure basically shows the effect of yawing motion on base pressure. Experimental results of Reference 5, for a projectile shape with and without a boattail but no base injection, show that the base pressure decreases with increasing angle of attack and, therefore, has the same qualitative behavior as the flight data.

Some of the pressure data were filtered twice to effectively provide a band pass filter. Low pass filtering at 250 Hz removed some of the high frequency noise and high pass filtering above 40 Hz removed the lower frequency trends including those of the fast mode coning frequency. The remaining oscillatory data are primarily due to projectile spin. Figure 20 shows the filtered base flat pressure for a short time segment. Pressure oscillations are fairly well defined, if the amplitude is not too small, and the frequency is very close to the nose cone pressure frequency as shown in Figure 21 . These base pressure oscillations would seem to be an indication of the instantaneous gradient on the base. It is interesting to note that amplitude of the base pressure oscillation becomes larger when the nose cone pressure indicates a small projectile yaw angle. Circumferentially, the base flat pressure tap location is approximately 180 degrees from the nose cone pressure. When the base pressure oscillation is well defined, it generally seems to be 180 degrees out of phase with respect to the nose cone pressure.

Figure 22 shows a similar comparison between the nose cone pressure and the pressure at the base corner. The pressure at the base corner was at approximately the same circumferential location as the nose cone pressure and the two pressures generally seem to be in phase. The two base pressure taps are 180 degrees apart with respect to the center of the base but are at different radial locations. When the two base pressures are compared to each other as shown in Figure 23 , they appear to be 180 degrees out of phase when the oscillations are well defined. These observations indicate that the pressure at a location on the base which is closer to the windward side of the projectile, exhibits the higher pressures.

It is of interest to note in Figure 23 that the oscillations on the base flat are larger in amplitude than those at the base corner. The pressure tap at the base corner lies in a recessed area which may be in an region of secondary circulation and effectively shielded from the dynamic forces in the primary recirculating region. The secondary recirculating region would be annular in shape and provide a path for pressure signals from the windward to leeward side and, therefore, reduce the pressure difference. These speculations are provided as a possible explanation for the smaller amplitude of the oscillation at the base corner.

The data which illustrate the effects of projectile motion have been shown for only the initial part of the flight and the Mach number was in the range of 1.20 to 1.30. The effects of projectile motion at the later segments of the flight should be, but have not yet been, examined.

The accuracy of the absolute value of pressure measurements is difficult to determine. Bench test measurements indicated accuracies to within 0.5% but other factors such as instrument calibrations in the data retrieval process could possibly double the bench test error. Comparisons of data under different circumstances appear consistent with estimated errors on the order of 1% for absolute pressure.

The accuracy of the oscillating components of pressure, based on the amplitude of the oscillation, also needs to be considered. A simple experiment was conducted using the ground test spin fixture to determine the difference in time between a pressure pulse on the model surface and the time when the pulse was sensed by the transducer. A small air jet

was directed toward the projectile base as the model was spinning. A small reflector was also placed on the model from which reflected light was sensed. As the model was brought up to different spin rates, the phase shift between pressure and the reflected light signals provided the data needed to determine the time lag. The result of the experiment was that lag time was very nearly equal to the length of the pressure path divided by the speed of sound. The path lengths for the two base pressures and the nose cone pressure are: base corner - 0.20m; base flat - 0.15m; nose cone - 0.05m. If the model is spinning at 143 Hz and the pressure is assumed to be sinusoidal, the pressure would be at or above a given level for the length of the response time. For the three path lengths just considered, the pressure level would be, respectively, 0.966, 0.980, and 0.998 times the oscillation amplitude or greater. This analysis suggests a 2-3% attenuation for the base pressures and a negligible attenuation for the nose cone pressure. The corresponding phase lag for the three path lengths are, respectively, 29 degrees, 23 degrees, and 7 degrees. The nose cone oscillations, which are modulated by the fast mode coning motion, follow well behaved patterns and would seem to indicate that the accuracy is within 5% of the transient component. The amplitude of the base pressure oscillations are more erratic and more analysis or more data are needed to quantify the accuracy.

The primary objective of this test program was to obtain base pressure information. In order to evaluate the effectiveness of base burn gases on drag reduction more accurately, flight experiments should be made without base burn propellant. Although it is beyond the scope of this test program, a comprehensive aerodynamic package could be extracted from the results of the flight data. Radar data provide trajectory and Mach number information; nose cone pressures provide frequency and amplitude of the yawing motion (nose cone pressures must be related to yaw angle with aid of theory or experiment). One flight provides data for the entire Mach number range of the trajectory. The cost of an instrumented round is not inexpensive, but numerous experiments in ground test facilities would be required to duplicate the data that could be acquired in a single flight.

IV. Conclusions

1. The test projectile had the same external shape as the M864, but the mass and inertial properties did not match those of the M864. The gyroscopic stability was adequate and a stable flight was achieved.

2. Base pressures and chamber pressure were successfully measured and the transducers were adequately protected from the high pressure gun gases.

3. These bases pressure measurements are believed to be the first obtained on projectile base during flight and propellant burning.

4. The effects of slowly varying parameters such as Mach number, altitude, and projectile yawing motion appear to be accurately measured.

5. The effects of spin, which produce pressure oscillations of approximately 140 hz, are qualitatively measured.

6. The chamber temperature measurements show erratic behavior and generally do not reflect the actual gas temperature. The measurements do provide some bounds on the temperature and the thermocouple responds to certain events. Therefore, temperature measurements do provide useful data.

7. The nose cone pressures provide projectile yawing motion data and the instantaneous windward-leeward orientation and are essential to understanding of the transient components of the base pressure.

8. The data are valuable for evaluating computational codes and for development of analytical or empirical models.

9. To effectively evaluate base burn effects, flight test data without propellant gas injection are needed.

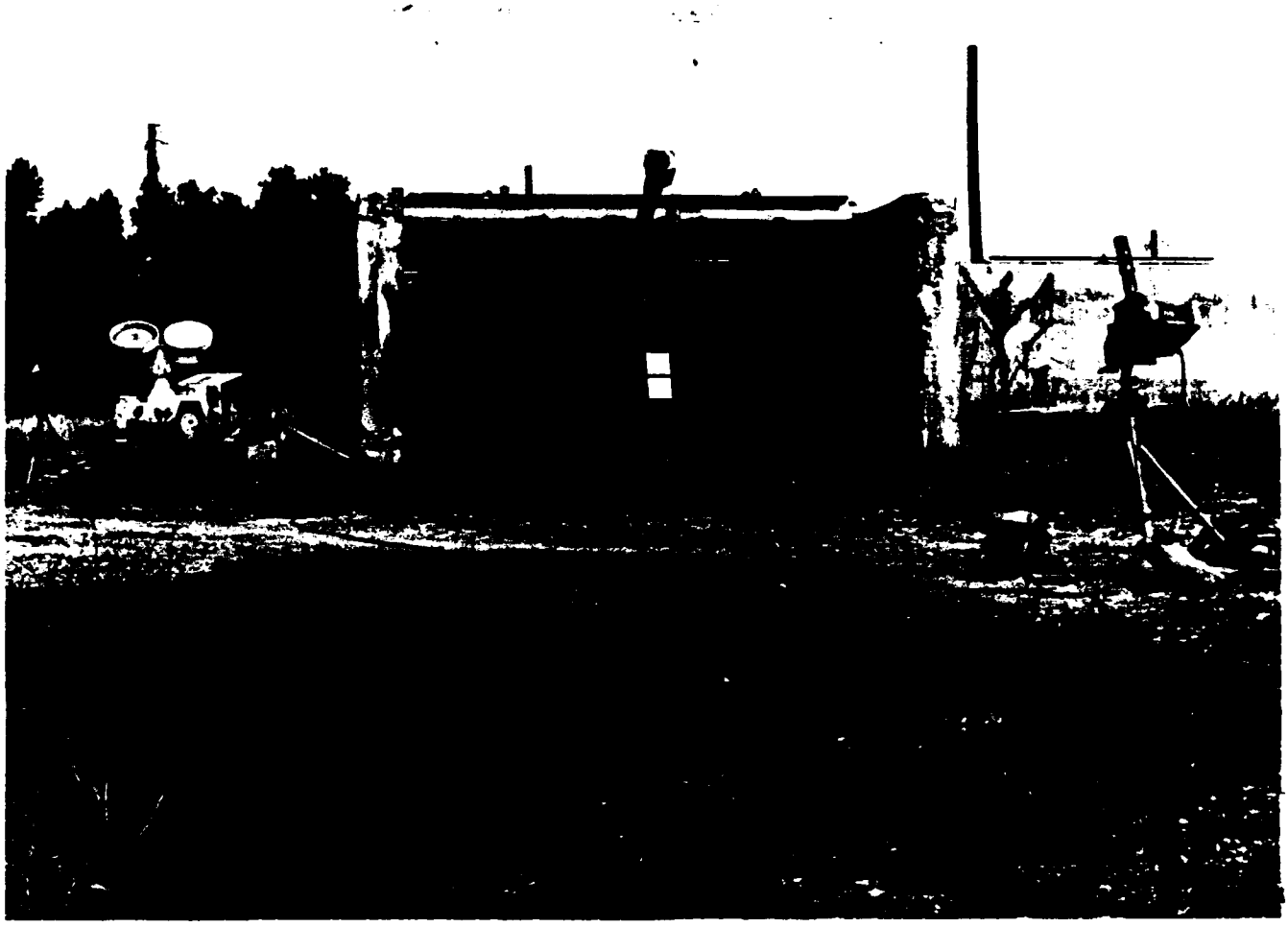

Figure 1. Gun System and Other Experimental Apparatus

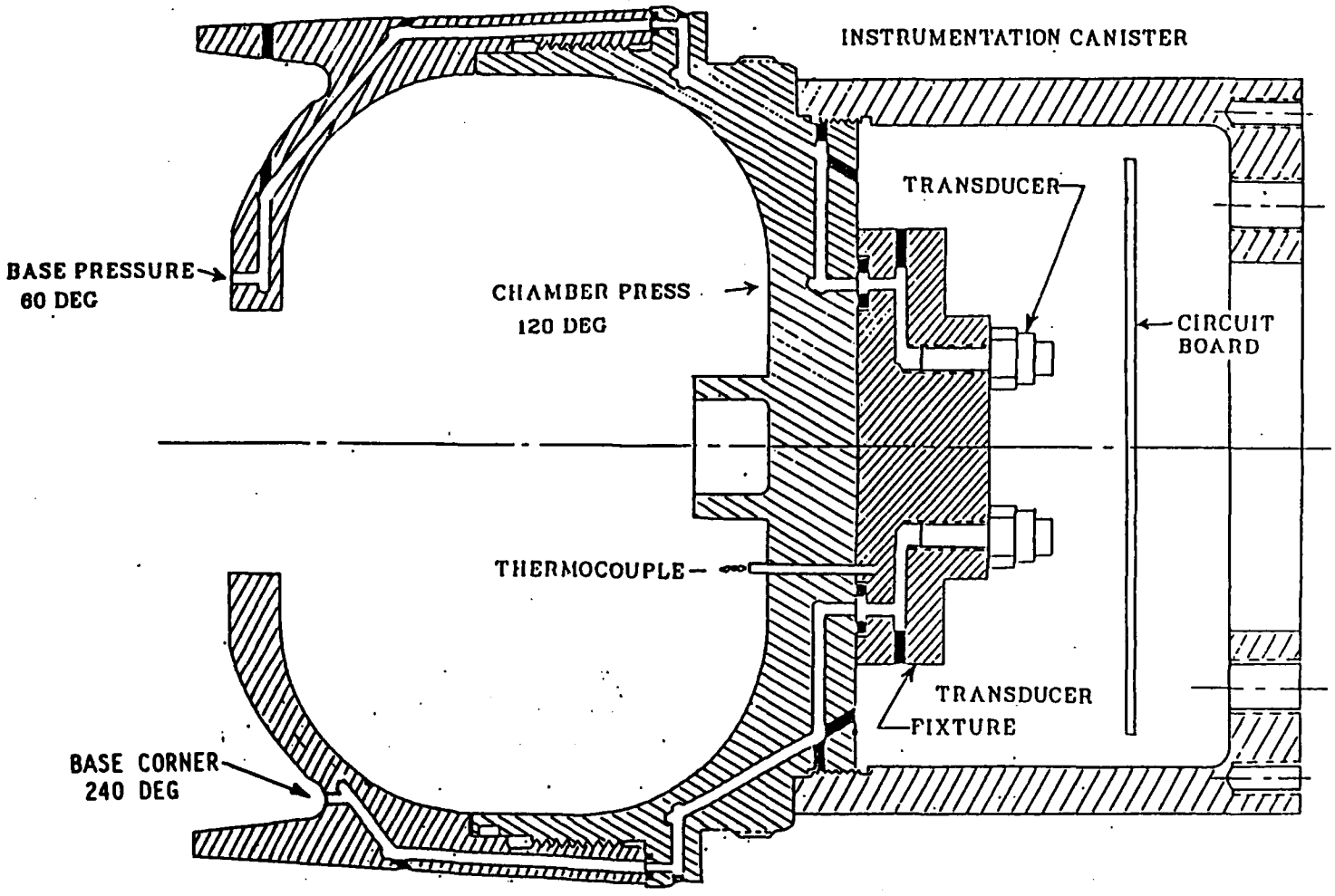

Figure 2. Projectile Base Pressure Ports and Instrumentation Canister

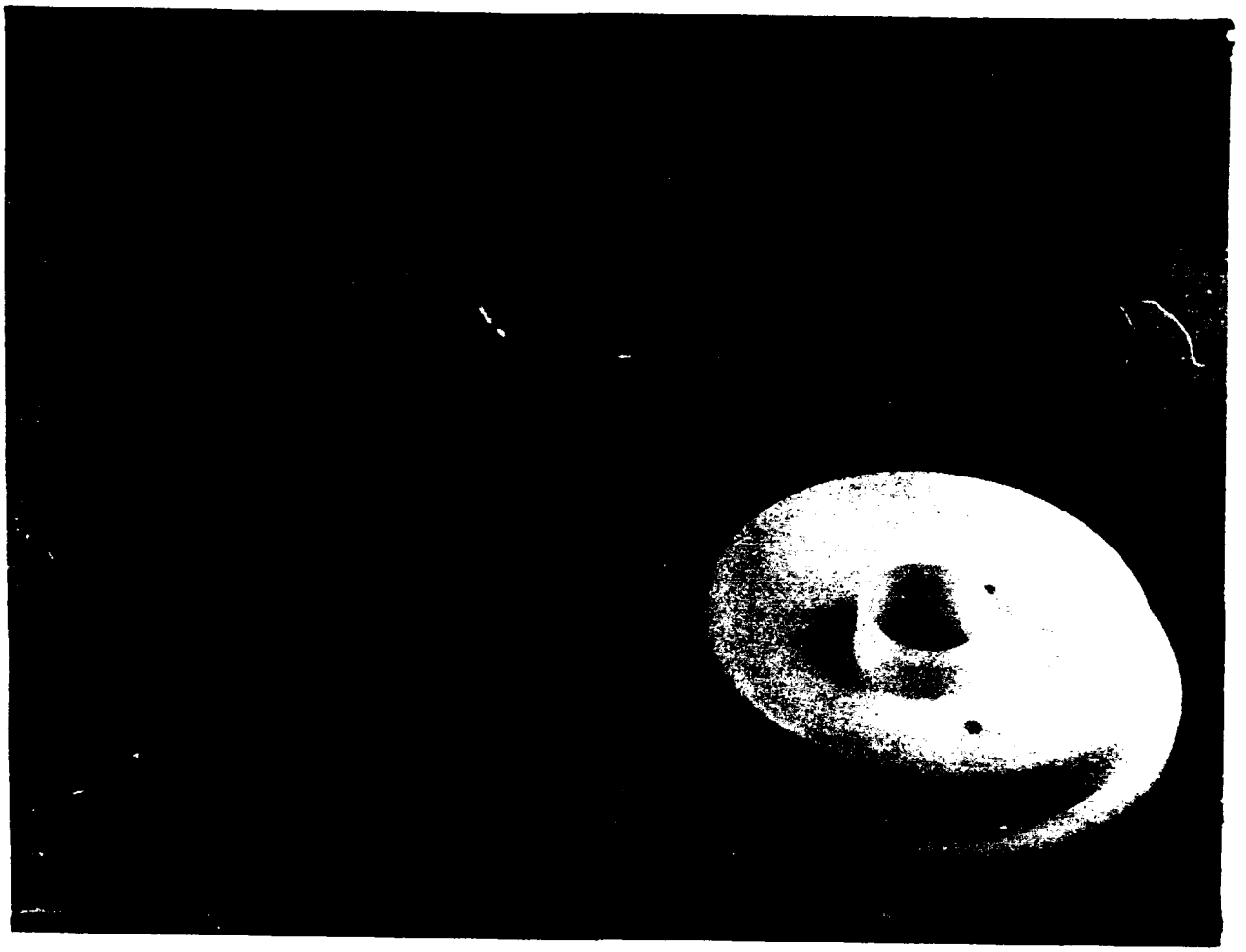

Figure 3. Projectile Base, Pusher Plate, and RTV Seal

Figure 4. Photograph of the M864 Propellant Grain

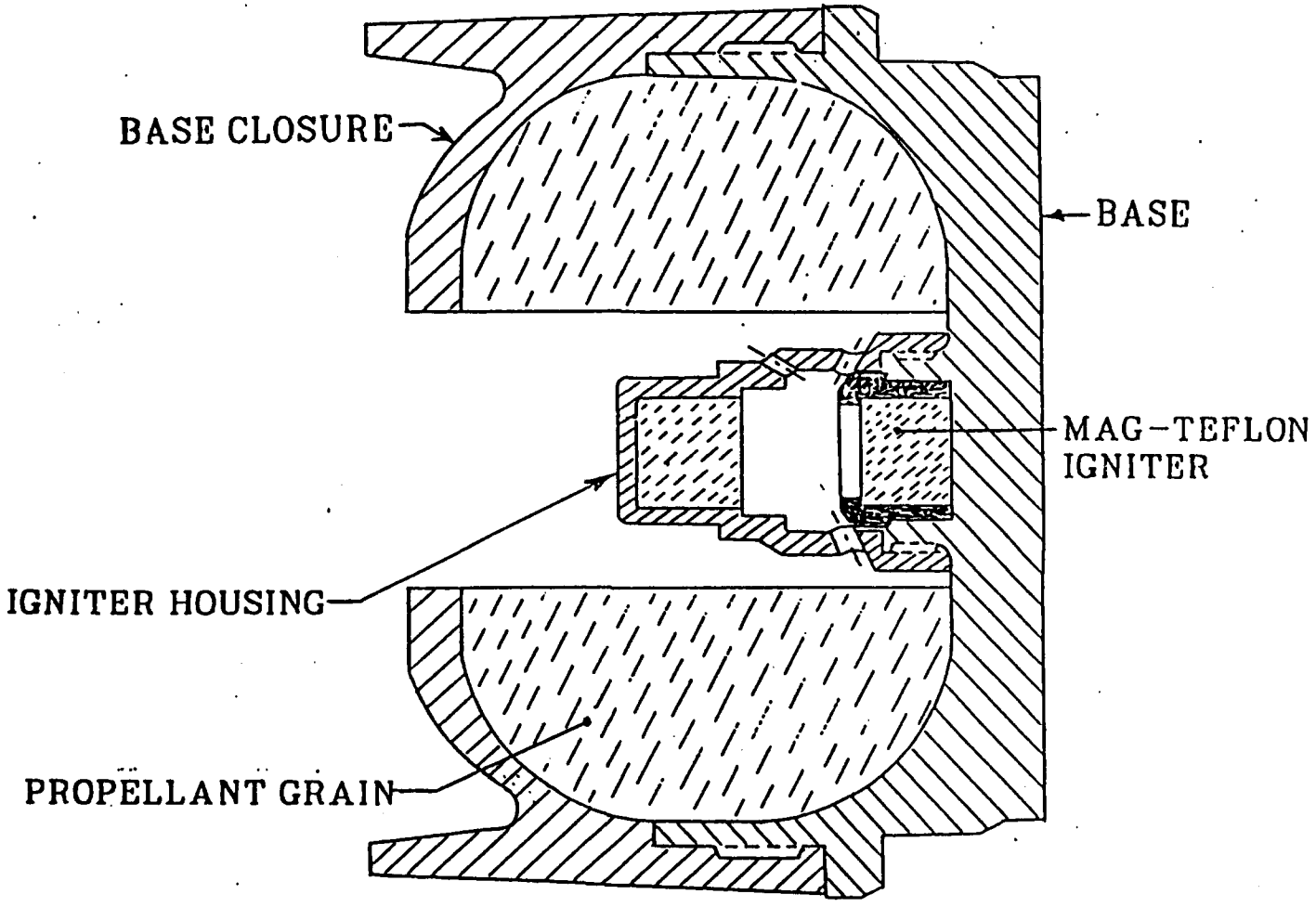

Figure 5. M864 Propellant Grain and Ignitor Installation

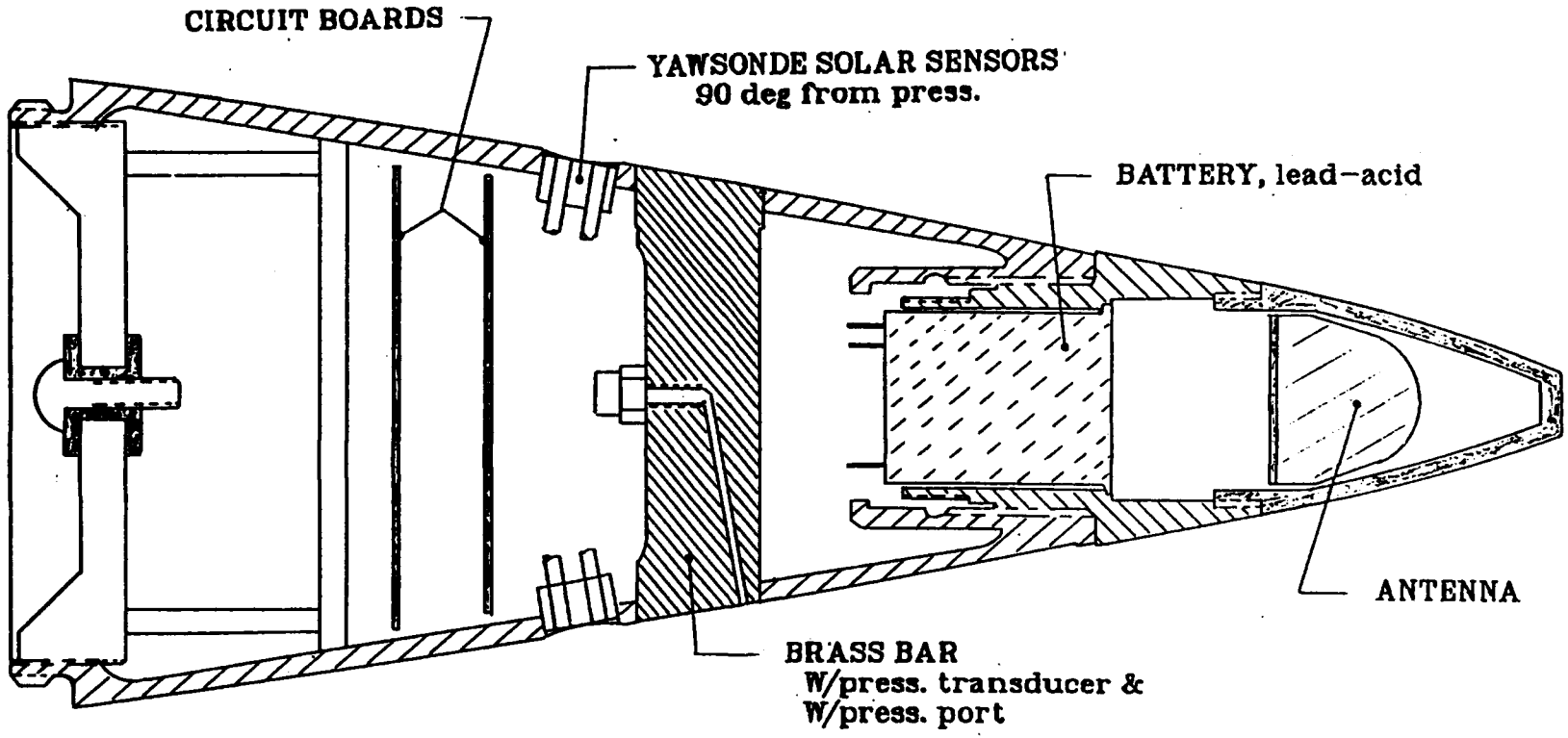

Figure 6. Instrumentation at the Nose of the Projectile

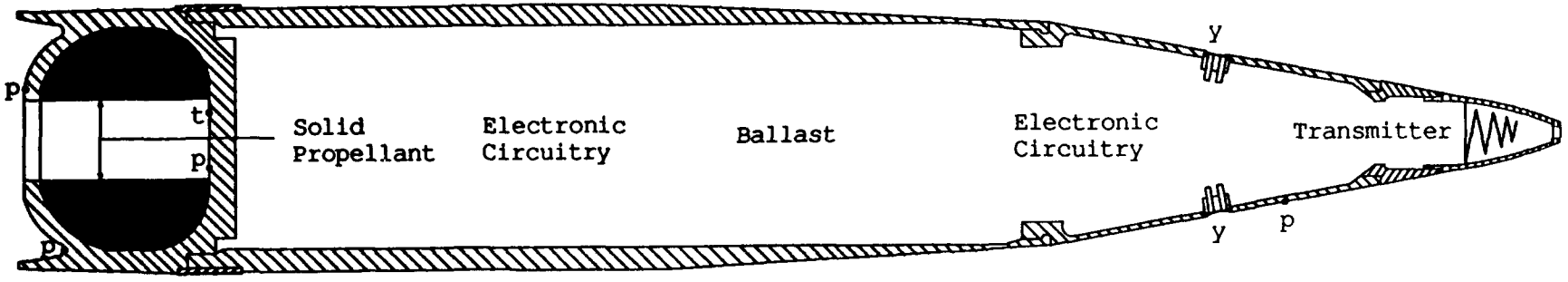

Figure 7. Schematic of the Instrumented Base-Burn Projectile

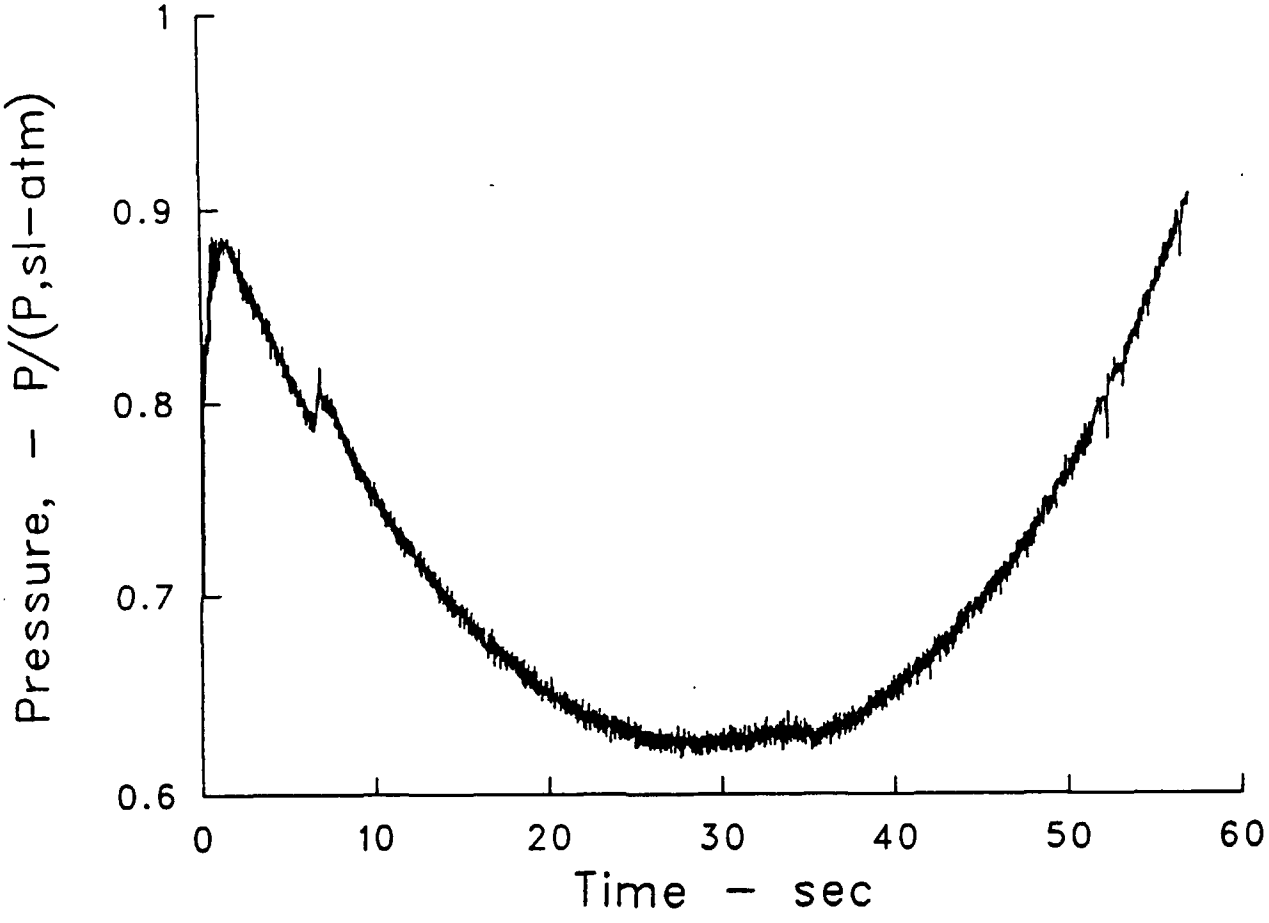

Figure 8. Base Corner Pressure, Unfiltered

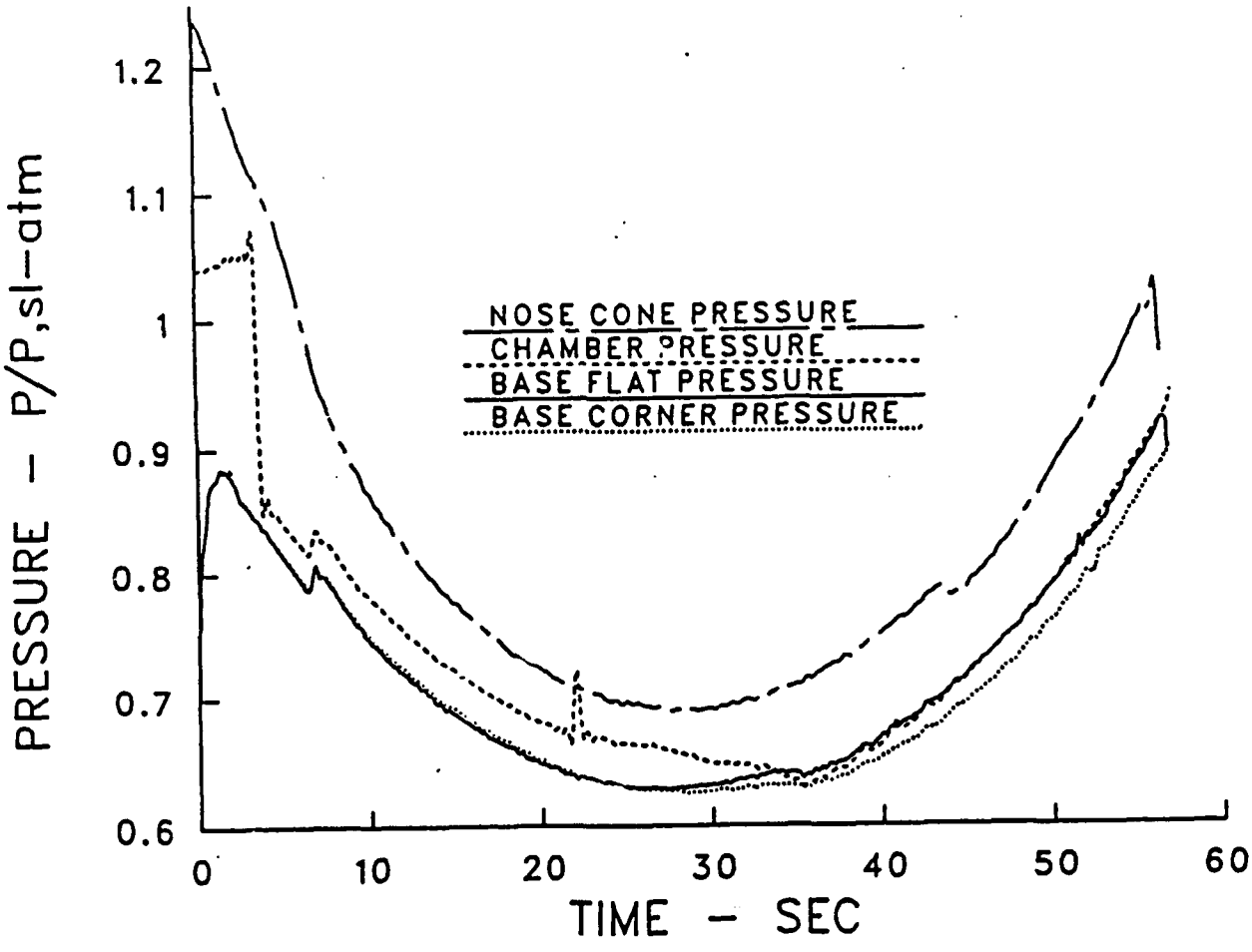

Figure 9. Base Corner, Flat; Chamber; and Nose Pressures, Filtered

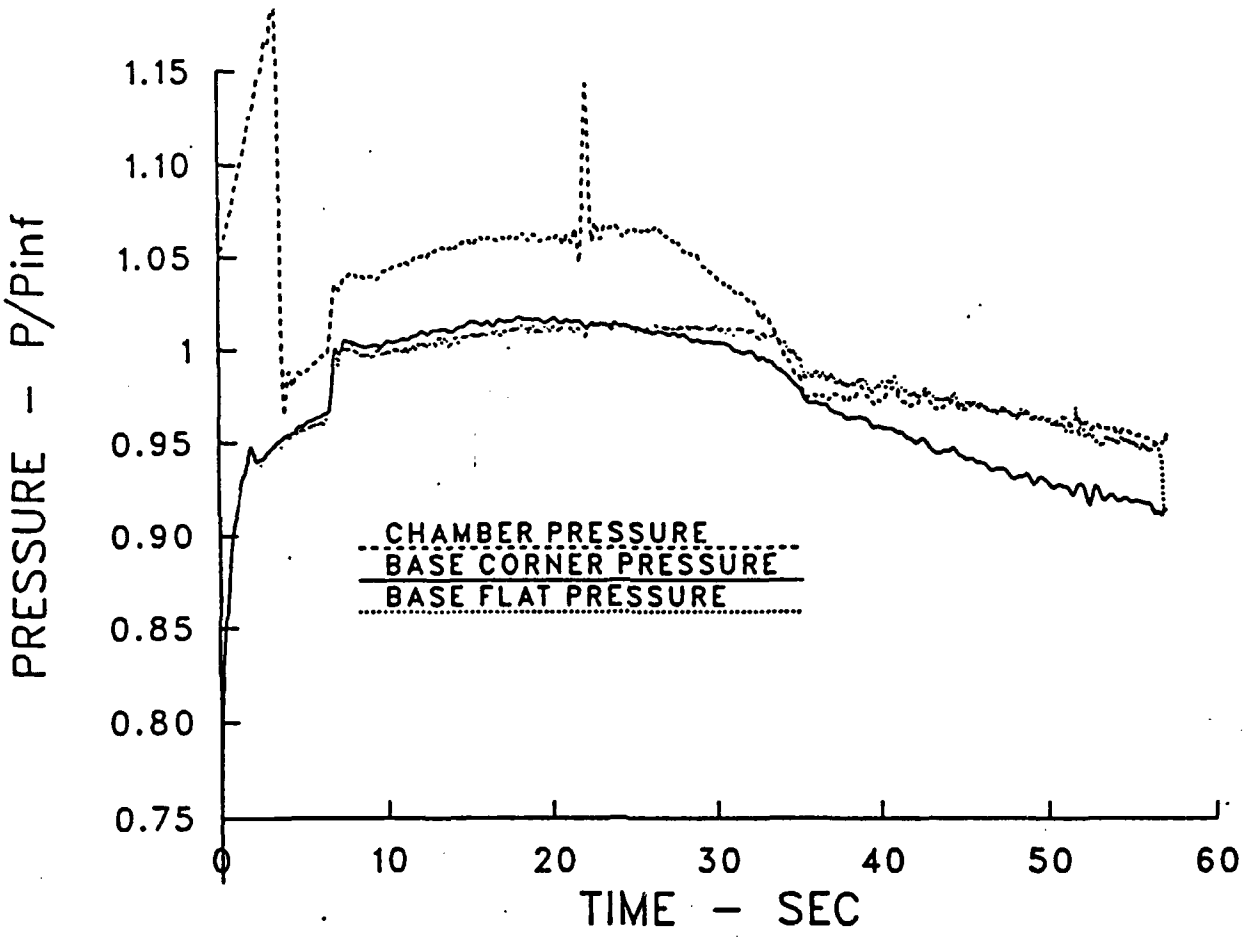

Figure 10. Base Corner, Base Flat, and Chamber Pressures (P/P_∞)

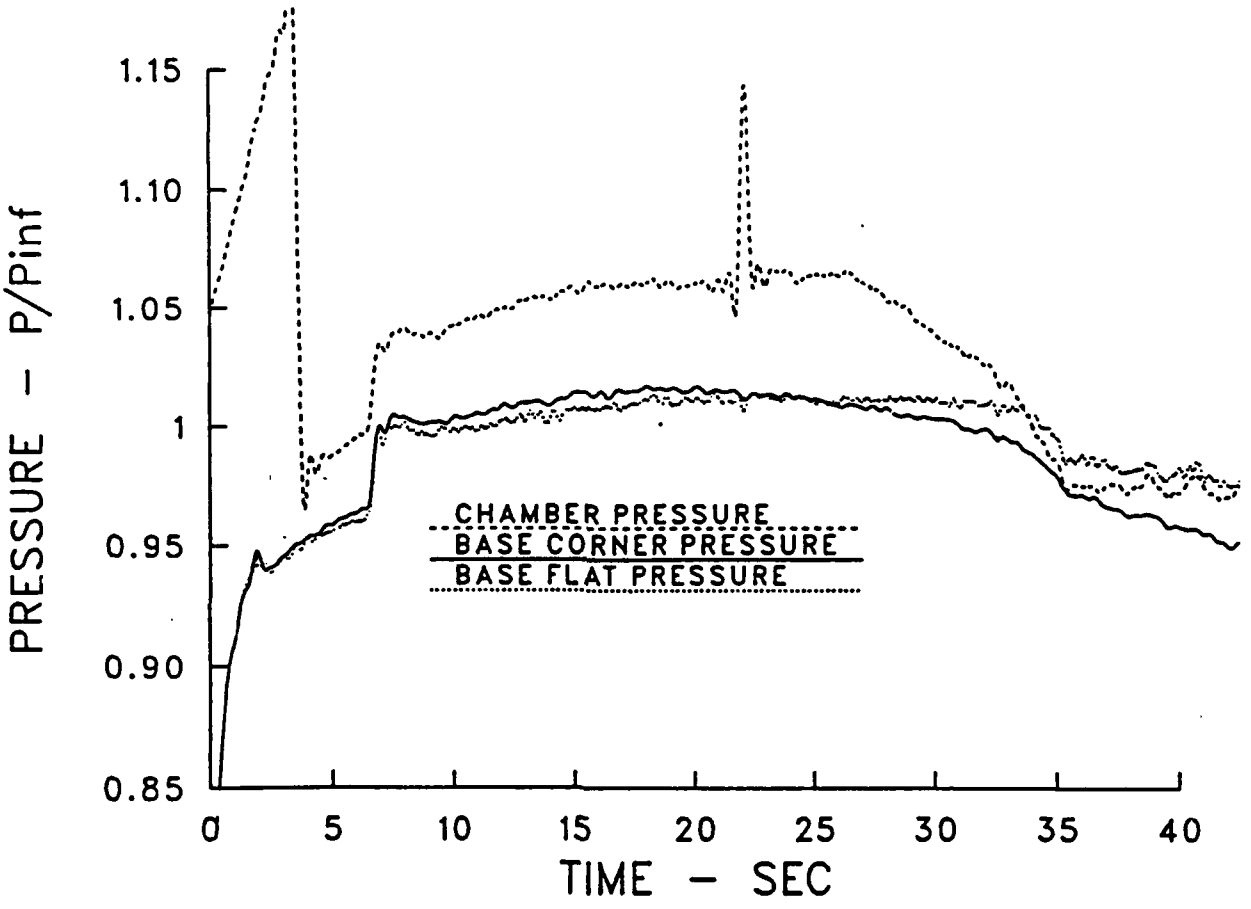

Figure 11. Base Corner, Base Flat, and Chamber Pressures (P/P_∞); Expanded

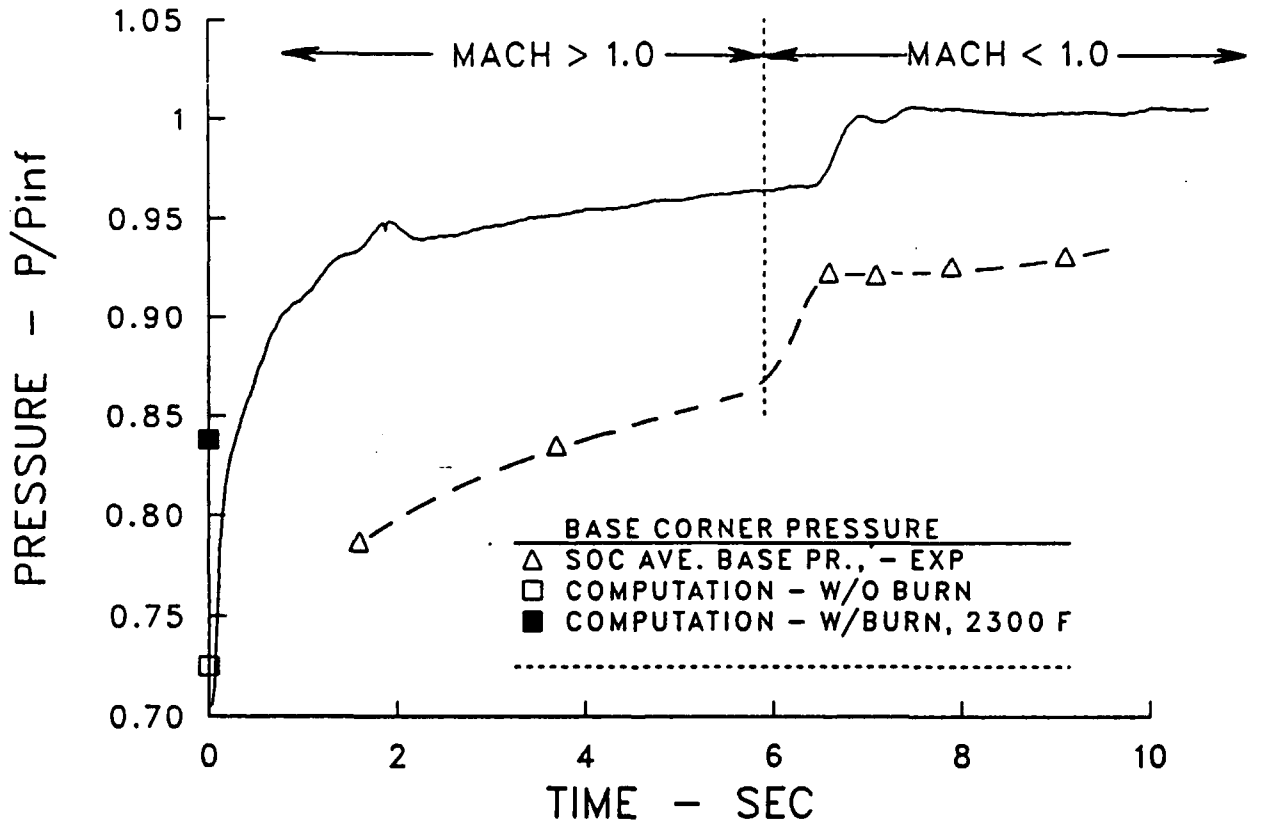

Figure 12. Comparison of Base Pressure with Other Data

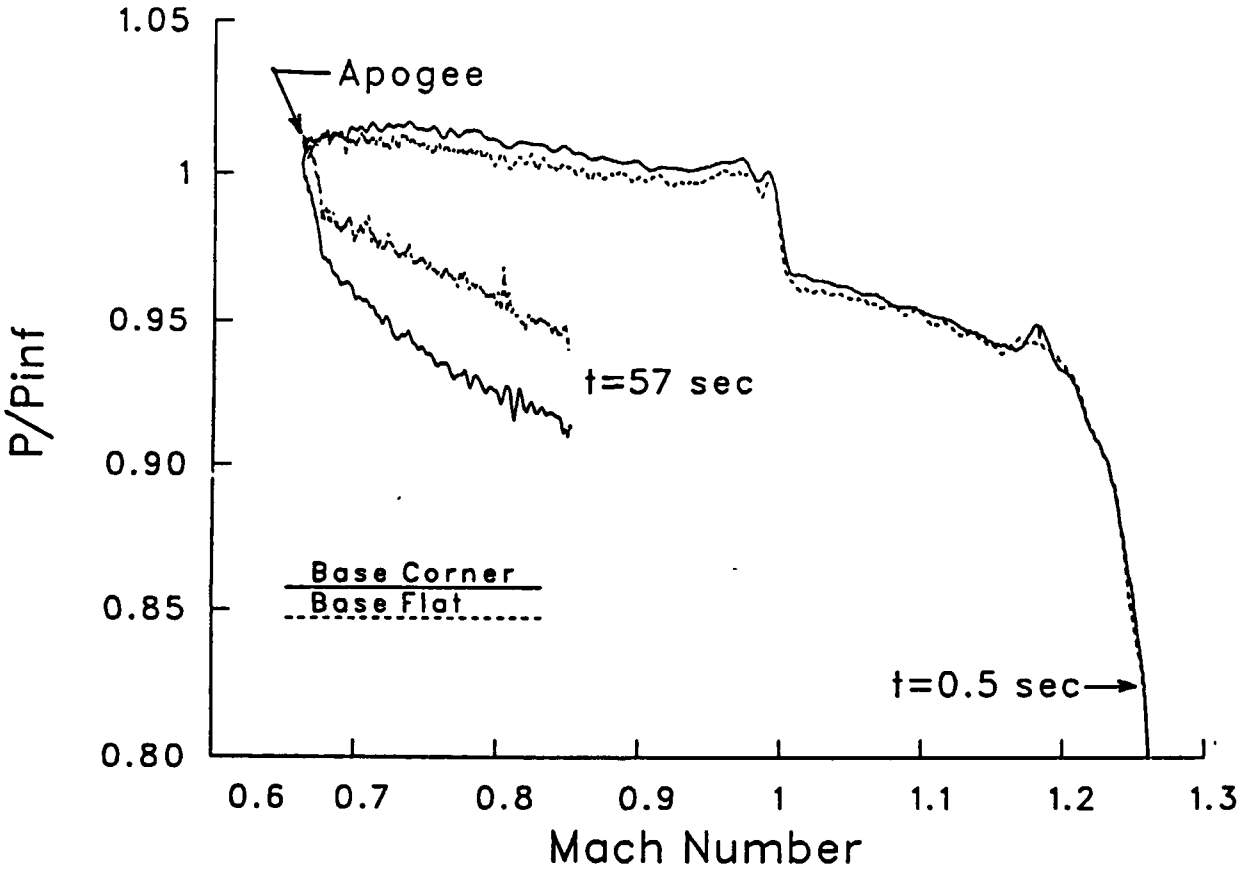

Figure 13. Base Corner and Base Flat Pressures versus Mach Number

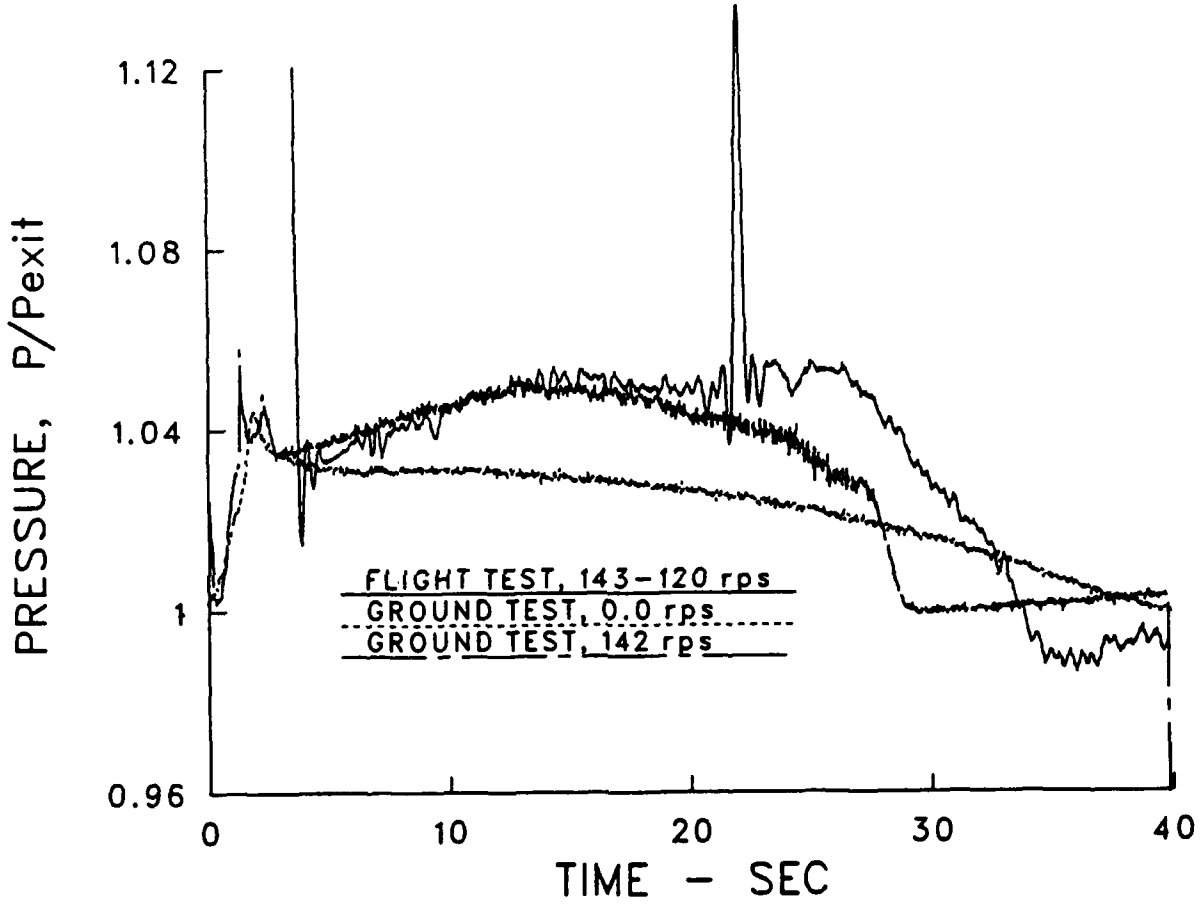

Figure 14. Chamber Pressure Measurements, Flight and Ground Tests

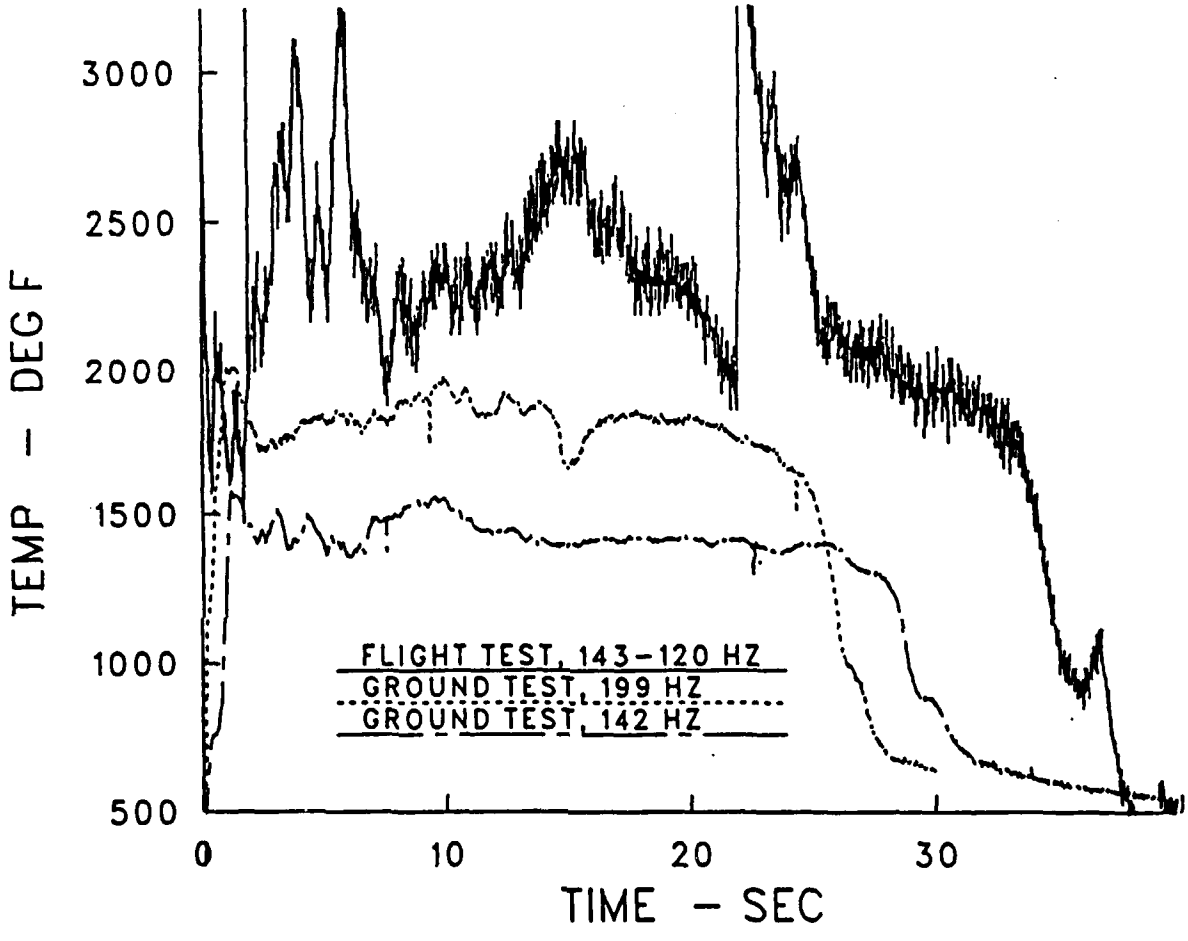

Figure 15. Temperature Measurements, Flight and Ground Tests

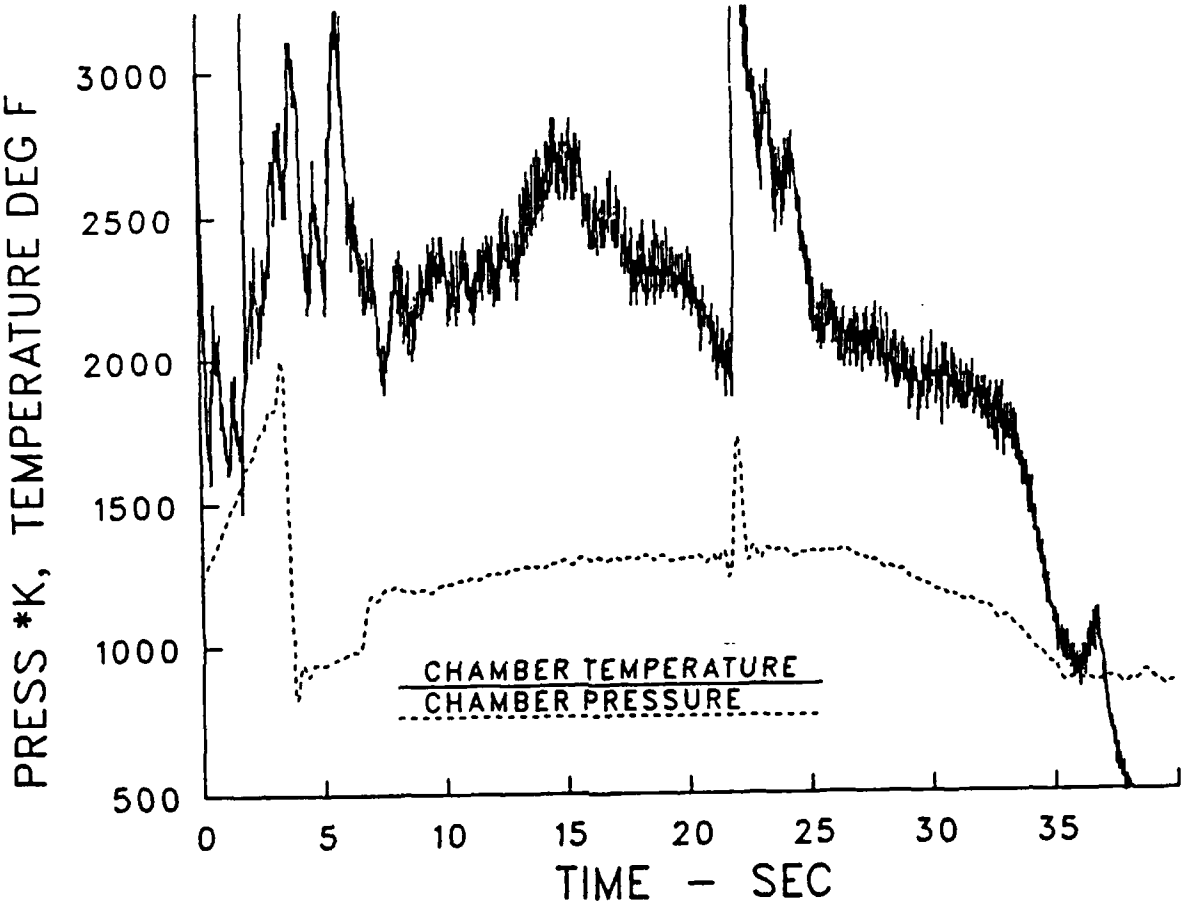

Figure 16. Comparison of Temperature and Pressure Measurements

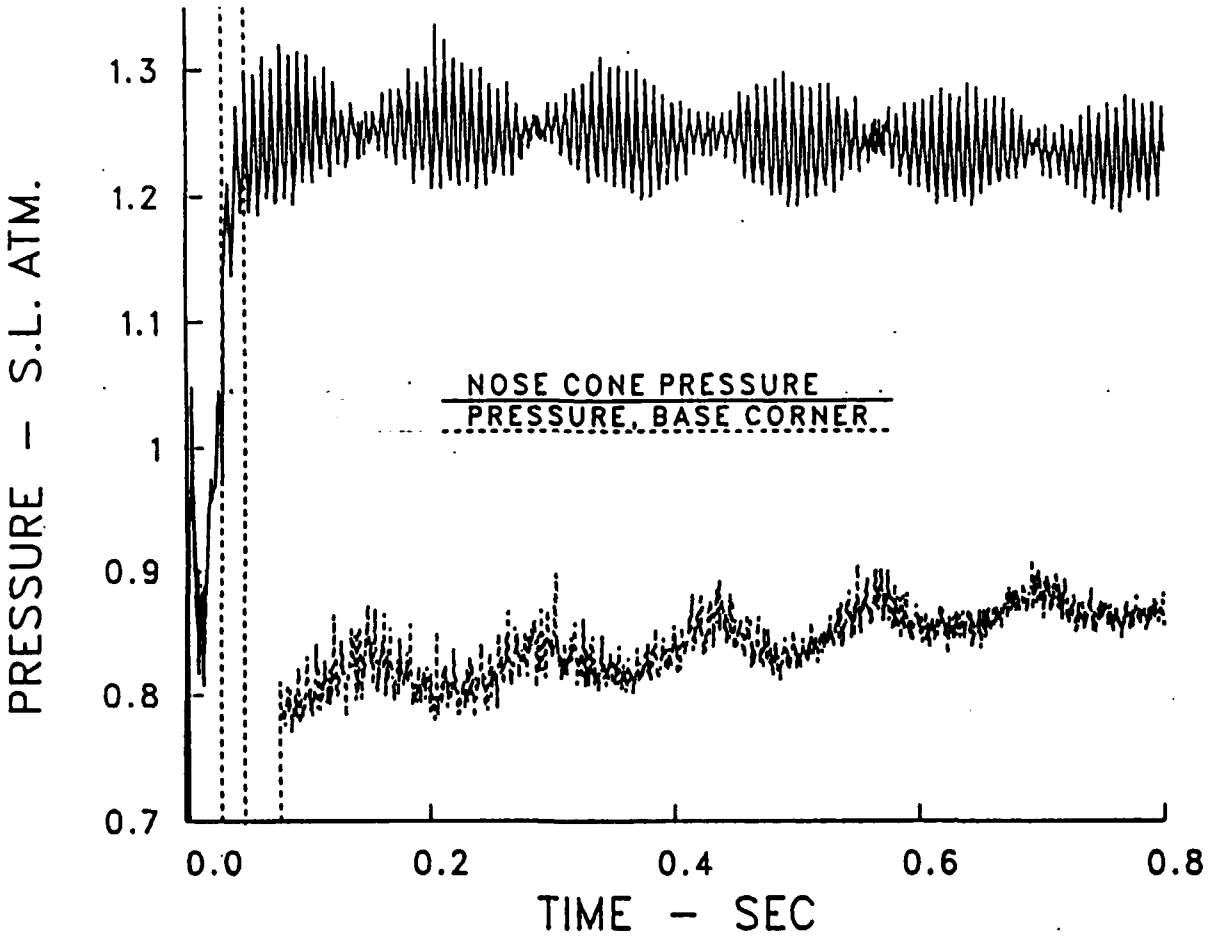

Figure 17. Effect of Projectile Yawing Motion on Pressure

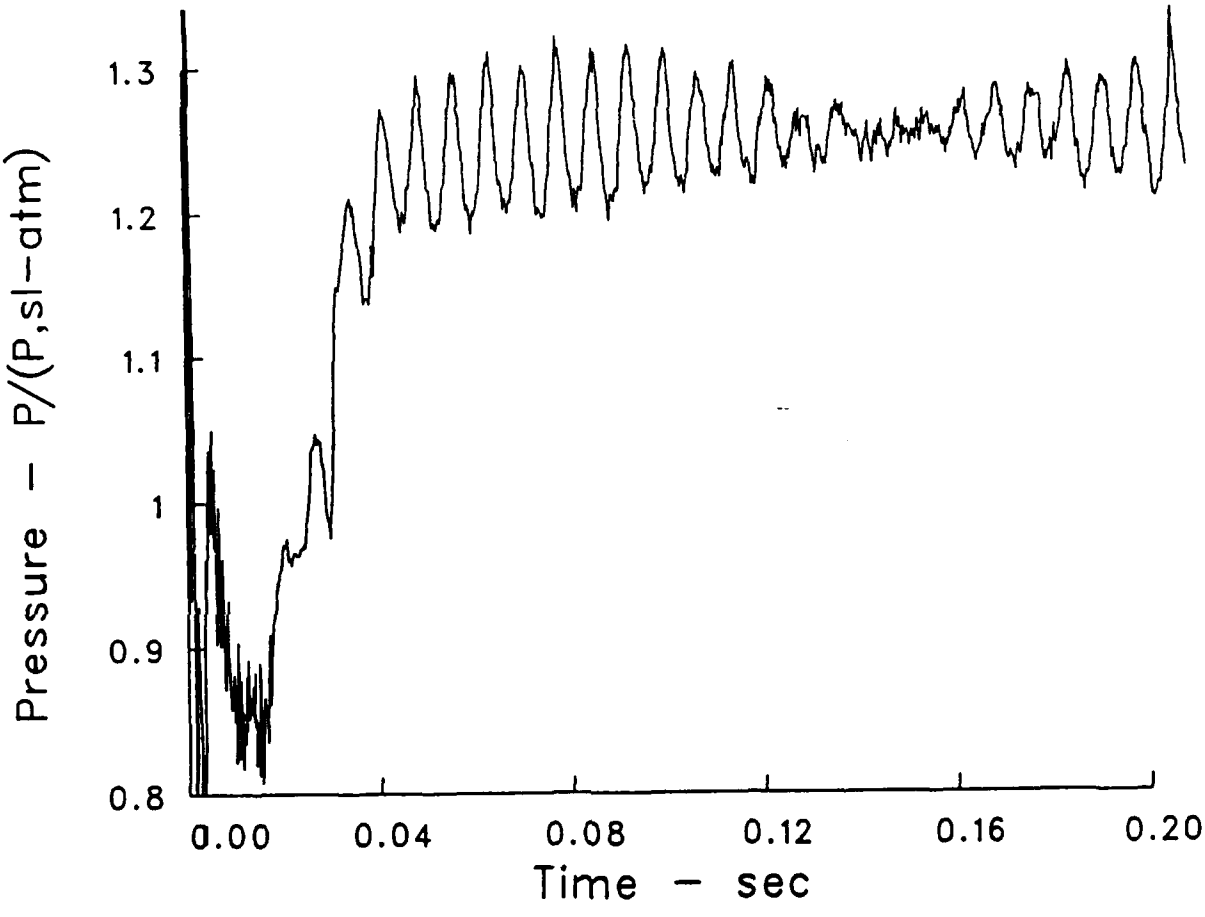

Figure 18. Nose Cone Pressure, First 0.2 Second

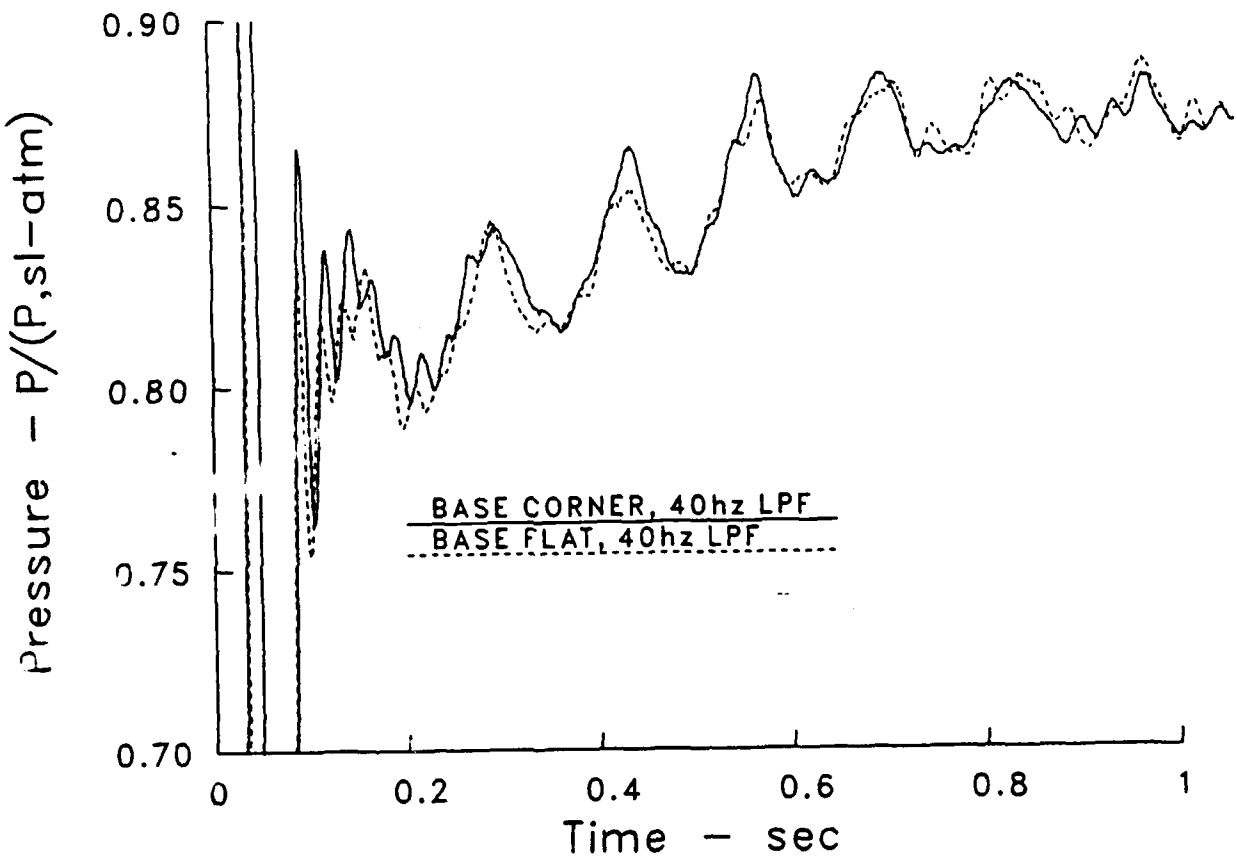

Figure 19. Filtered Base Corner and Base Flat Pressures

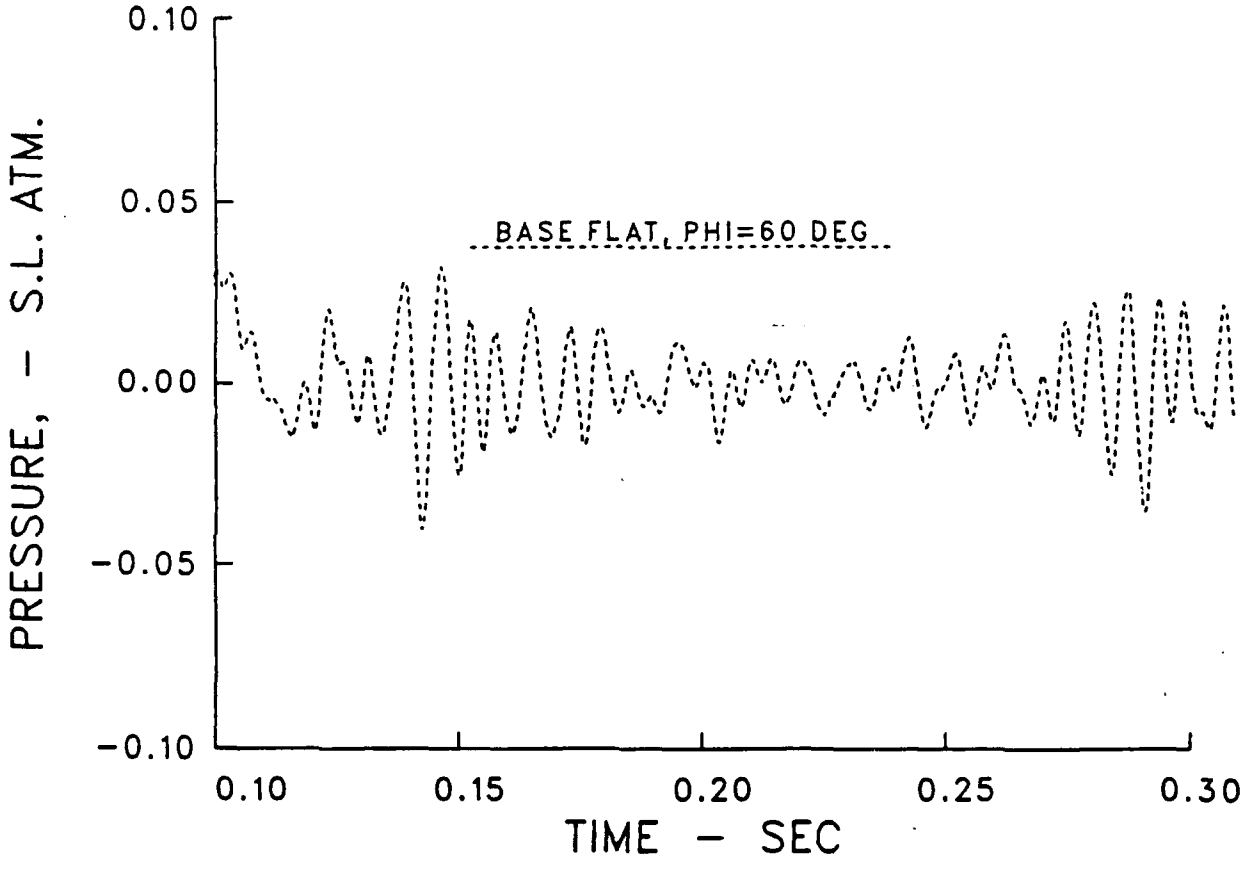

Figure 20. Filtered Base Flat Pressure, 0.1 to 0.3 Second

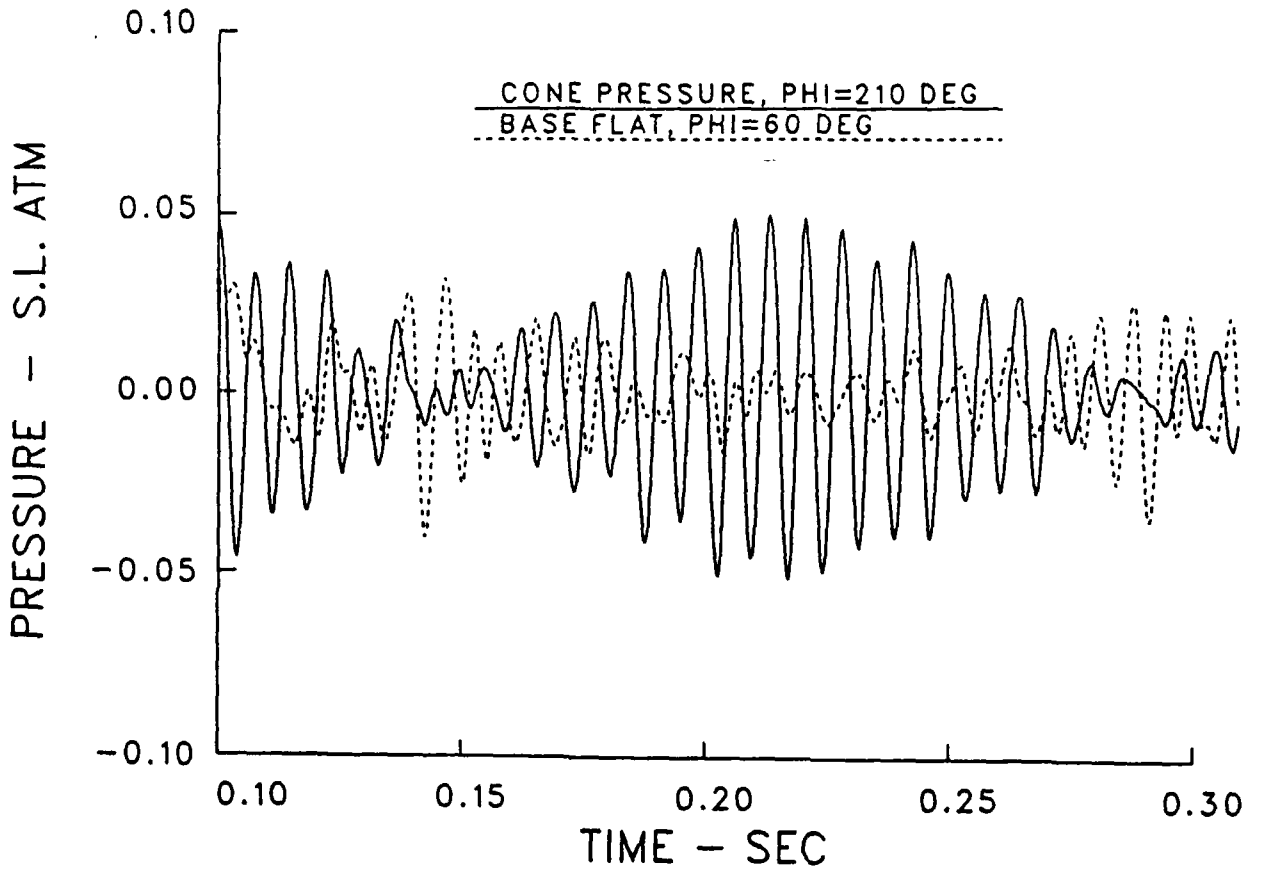

Figure 21. Filtered Nose Cone and Base Flat Pressures, 0.1 to 0.3 Second

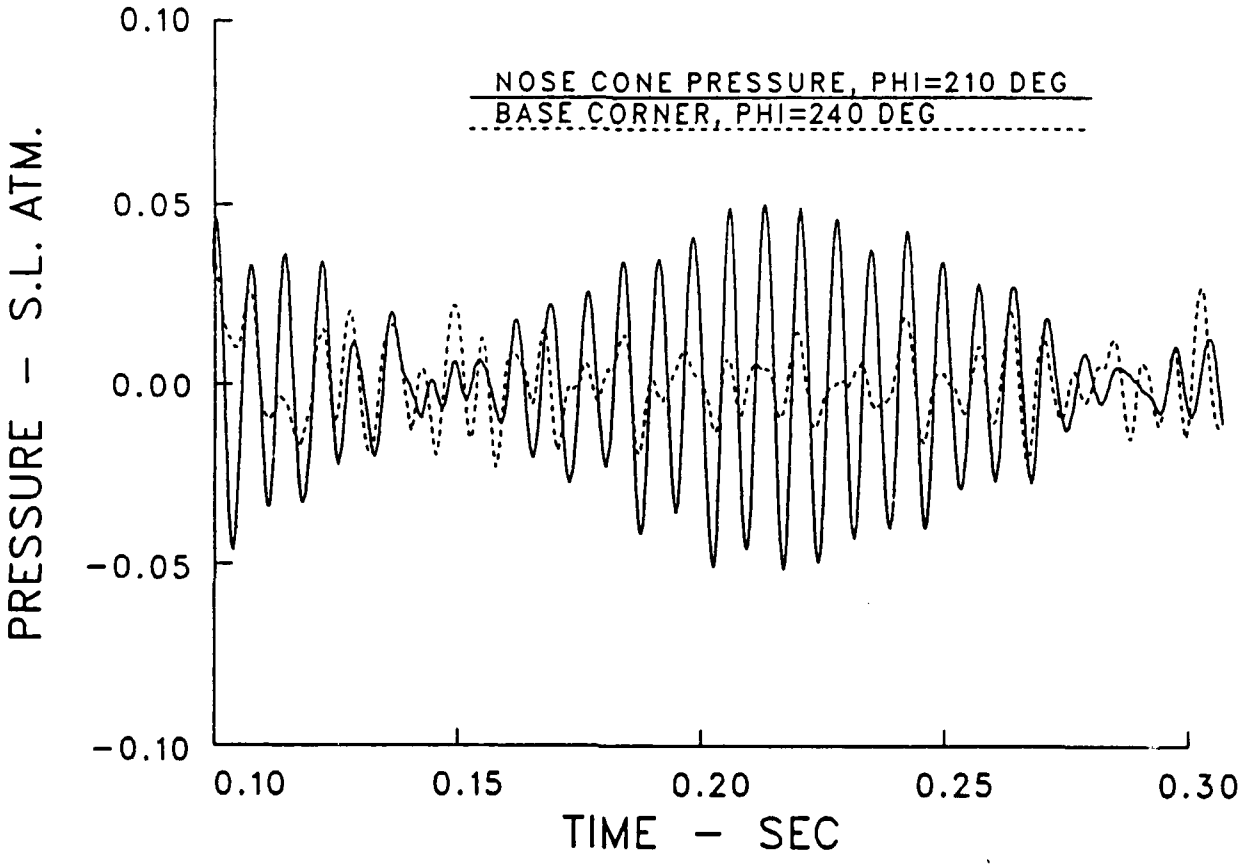

Figure 22. Filtered Nose Cone and Base Corner Pressures, 0.1 to 0.3 Second

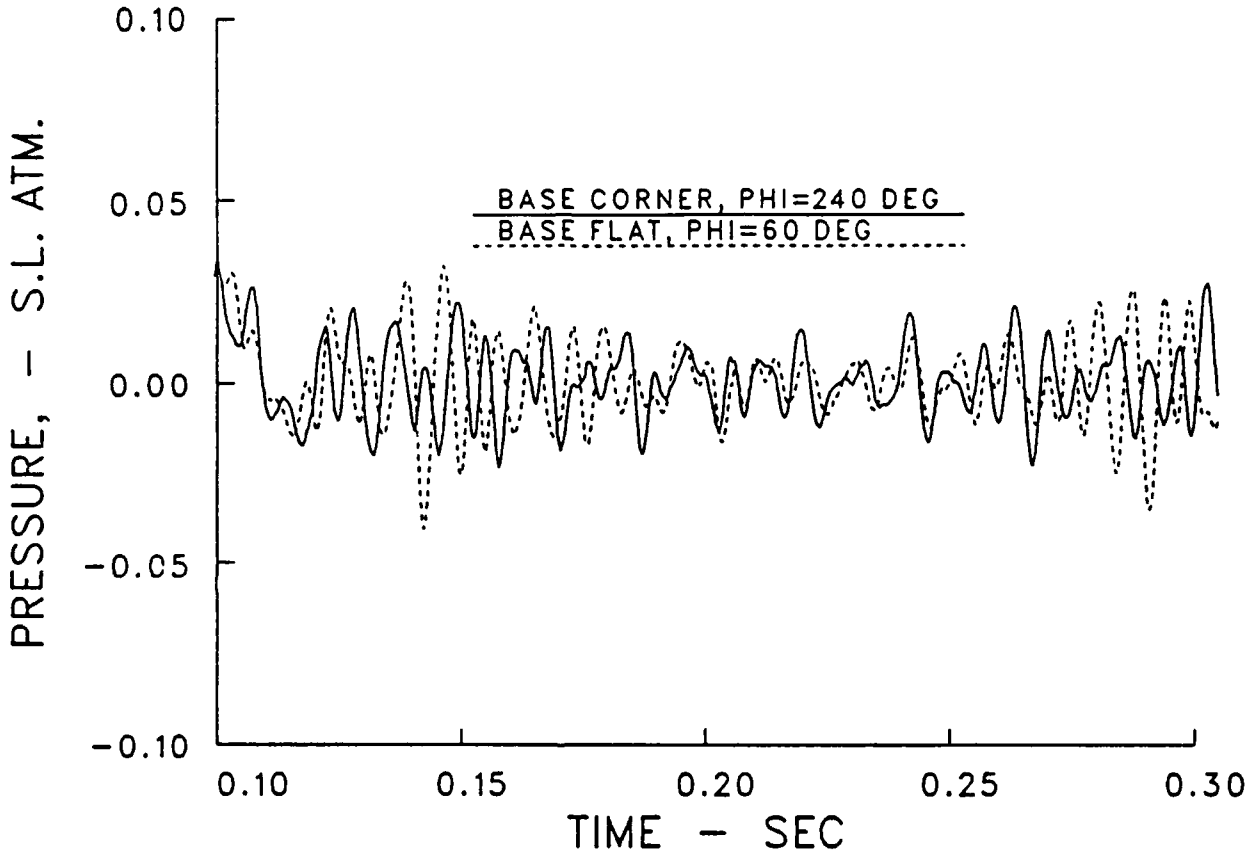

Figure 23. Filtered Base Flat and Base Corner Pressures, 0.1 to 0.3 Second

INTENTIONALLY LEFT BLANK.

No of Copies	Organization
1	Office of the Secretary of Defense OUSD(A) Director, Live Fire Testing ATTN: James F. O'Bryon Washington, DC 20301-3110
2	Administrator Defense Technical Info Center ATTN: DTIC-DDA Cameron Station Alexandria, VA 22304-6145
1	HQDA (SARD-TR) WASH DC 20310-0001
1	Commander US Army Materiel Command ATTN: AMCDRA-ST 5001 Eisenhower Avenue Alexandria, VA 22333-0001
1	Commander US Army Laboratory Command ATTN: AMSLC-DL Adelphi, MD 20783-1145
2	Commander US Army, ARDEC ATTN: SMCAR-IMI-I Picatinny Arsenal, NJ 07806-5000
2	Commander US Army, ARDEC ATTN: SMCAR-TDC Picatinny Arsenal, NJ 07806-5000
1	Director Benet Weapons Laboratory US Army, ARDEC ATTN: SMCAR-CCB-TL Watervliet, NY 12189-4050
1	Commander US Army Armament, Munitions and Chemical Command ATTN: SMCAR-ESP-L Rock Island, IL 61299-5000
1	Commander US Army Aviation Systems Command ATTN: AMSAV-DACL 4300 Goodfellow Blvd. St. Louis, MO 63120-1798

No of Copies	Organization
1	Director US Army Aviation Research and Technology Activity Ames Research Center Moffett Field, CA 94035-1099
1	Commander US Army Missile Command ATTN: AMSMI-RD-CS-R (DOC) Redstone Arsenal, AL 35898-5010
1	Commander US Army Tank-Automotive Command ATTN: AMSTA-TSL (Technical Library) Warren, MI 48397-5000
1	Director US Army TRADOC Analysis Command ATTN: ATAA-SL White Sands Missile Range, NM 88002-5502
(Class. only) 1	Commandant US Army Infantry School ATTN: ATSH-CD (Security Mgr.) Fort Benning, GA 31905-5660
(Unclass. only) 1	Commandant US Army Infantry School ATTN: ATSH-CD-CSO-OR Fort Benning, GA 31905-5660
1	Air Force Armament Laboratory ATTN: AFATL/DLODL Eglin AFB, FL 32542-5000
	Aberdeen Proving Ground
2	Dir, USAMSAA ATTN: AMXSY-D AMXSY-MP, H. Cohen
1	Cdr, USATECOM ATTN: AMSTE-TD
3	Cdr, CRDEC, AMCCOM ATTN: SMCCR-RSP-A SMCCR-MU SMCCR-MSI
1	Dir, VLAMO ATTN: AMSLC-VL-D

DISTRIBUTION

No. of Copies	Organization
2	Commander US Army AMCCOM Project Manager - Howitzer Improvement Program ATTN: AMCPM-HIP R. Kantenwein R. DeKleine Picatinny Arsenal, NJ 07806-5000
2	Project Manager Autonomous Precision-Guided Munitions (APGM) Armament RD&E Center US Army AMCCOM ATTN: AMCPM-APGM J. Williams D. Griggs Picatinny Arsenal, NJ 07806-5000
1	Commander US Army AMCCOM Program Executive Office for Armaments ATTN: AMCPEO-AR-M Mr. M. DellaTerga Picatinny Arsenal, NJ 07806-5000
3	Commander Armament RD&E Center US Army AMCCOM ATTN: SMCAR-FSA-M F. Brody R. Botticelli P. Demasi Picatinny Arsenal, NJ 07806-5000
2	Commander Armament RD&E Center US Army AMCCOM ATTN: SMCAR-AET-A R. Kline H. Hudgins Picatinny Arsenal, NJ 07806-5000
2	Commander Armament RD&E Center US Army AMCCOM ATTN: SMCAR-FSP-A F. Scerbo J. Bera Picatinny Arsenal, NJ 07806-5000

No. of Copies	Organization
1	Commander US Army Missile Command ATTN: AMSMI-RDK (W. Dahlke) Redstone Arsenal, AL 35898-5010
1	Commander Naval Surface Warfare Center ATTN: Dr. W. Yanta Aerodynamics Branch K-24, Bldg. 402-12 White Oak Laboratory Silver Spring, MD 20910
1	Director National Aeronautics and Space Administration Ames Research Center ATTN: Dr. J. Steger Moffett Field, CA 94035
1	Arizona State University Department of Mechanical and Energy Systems Engineering ATTN: Dr. G.P. Neitzel Tempe, AZ 85281
1	University of Santa Clara Department of Physics ATTN: R. Greeley Santa Clara, CA 95053

Aberdeen Proving Ground

Commander, CRDEC, AMCCOM
ATTN: SMCCR-RSP-A
M.C. Miller
D. Olson
SMCCR-MU
W. Dee
C. Hughes
D. Bromley

USER EVALUATION SHEET/CHANGE OF ADDRESS

This Laboratory undertakes a continuing effort to improve the quality of the reports it publishes. Your comments/answers to the items/questions below will aid us in our efforts.

1. BRL Report Number BRL-MR-3830 Date of Report April 1990

2. Date Report Received _____

3. Does this report satisfy a need? (Comment on purpose, related project, or other area of interest for which the report will be used.) _____

4. Specifically, how is the report being used? (Information source, design data, procedure, source of ideas, etc.) _____

5. Has the information in this report led to any quantitative savings as far as man-hours or dollars saved, operating costs avoided, or efficiencies achieved, etc? If so, please elaborate. _____

6. General Comments. What do you think should be changed to improve future reports? (Indicate changes to organization, technical content, format, etc.) _____

CURRENT ADDRESS

Name

Organization

Address

City, State, Zip Code

7. If indicating a Change of Address or Address Correction, please provide the New or Correct Address in Block 6 above and the Old or Incorrect address below.

OLD ADDRESS

Name

Organization

Address

City, State, Zip Code

(Remove this sheet, fold as indicated, staple or tape closed, and mail.)

----------FOLD HERE----------

DEPARTMENT OF THE ARMY
Director
U.S. Army Ballistic Research Laboratory
ATTN: SLCBR-DD-T
Aberdeen Proving Ground, MD 21005-5066
OFFICIAL BUSINESS

NO POSTAGE
NECESSARY
IF MAILED
IN THE
UNITED STATES

BUSINESS REPLY MAIL
FIRST CLASS PERMIT No 0001, APG, MD

POSTAGE WILL BE PAID BY ADDRESSEE

Director
U.S. Army Ballistic Research Laboratory
ATTN: SLCBR-DD-T
Aberdeen Proving Ground, MD 21005-9989

----------FOLD HERE----------